Journal of Hydrology 590 (2020) 125403

Contents lists available at ScienceDirect

Journal of Hydrology

journal homepage: www.elsevier.com/locate/jhydrol

Research papers

Projecting impacts of wildfire and climate change on streamflow, sediment, and organic carbon yields in a forested watershed

Danielle Loiselle[a], Xinzhong Du[a], Daniel S. Alessi[a], Kevin D. Bladon[b], Monireh Faramarzi[a,*]

[a] Department of Earth and Atmospheric Sciences, University of Alberta, 1-26 Earth Sciences Building, Edmonton, AB T6G 2E3, Canada
[b] Department of Forest Engineering, Resources, and Management, Oregon State University, Corvallis, OR 97331, USA

ARTICLE INFO

Keywords:
SWAT-OSCM
Biogeochemical processes
Hydrological processes
Dissolved organic carbon
Particulate organic carbon

ABSTRACT

Increasing temperatures and irregular precipitation associated with climate change, along with increasing frequency and severity of wildfires, contribute to increased downstream transport of sediment and total organic carbon (TOC), with potential impacts on aquatic ecosystem structure and resilience, recreational use of water bodies, and downstream drinking water treatment. Our study aimed to investigate the effects of both climate change and wildfires on water budget, sediment, and organic carbon by simulating the response of sub-catchments and in-stream processes to changes in future climate and wildfire scenarios. To achieve this, we applied a physical process-based hydrologic model, where an in-stream Organic Carbon Simulation Module was embedded within the Soil and Water Assessment Tool (SWAT-OCSM), to the Elbow River watershed in Alberta, Canada. Post-wildfire conditions of both moderate and high burn severities were replicated in the model within two burn perimeters to assess in-stream organic carbon processes related to particulate organic carbon (POC) and dissolved organic carbon (DOC) as state variables under changing climate. Results of the climate change scenarios indicated lower streamflow relative to the baseline period (1995–2014), particularly between May–August, with 25.3–46.9% less water in the near future (2015–2034) compared to 9.9–31.8% less water in the distant future (2043–2062). Sediment concentrations generally decreased, whereas TOC concentrations increased, in both the near future and distant future scenarios reflecting uncertainty in climate effects on water quality. Wildfire simulations compounded with climate change significantly changed local hydrology, increasing surface runoff, sediment, and TOC transport by over 500% in some study sub-catchments. However, at the watershed outlet, sediment yields only increased up to 6.5% and TOC yields increased up to 13.1%. Burn severity invoked a stronger watershed response than burn area, and greater relative changes were observed for wildfires occurring with the worst-case climate change scenarios. This study provided a strong basis for analyzing watershed responses to potential future wildfires. However, recommendations are provided for further model developments to account for wildfire consequences and feedbacks with hydrological and biogeochemical processes.

1. Introduction

Climate change has increased the frequency, size, and severity of natural disturbance events such as wildfires, droughts, storms, and pest and pathogen outbreaks that drive hydrological processes and influence water quantity and quality (Seidl et al., 2017; Mahat et al., 2016; IPCC, 2013; Wang et al., 2015). In particular, the combination of hotter summers with higher frequencies of droughts and thunderstorms has favored the ignition of wildfires (Flannigan et al., 2005; Marlon et al., 2012), and their severity and frequency are projected to continue increasing (Coogan et al., 2019; Flannigan et al., 2005). Aggressive wildfire suppression in many parts of the world, including Western North America, has led to increased connectivity of fuel sources, thus increasing the risk of extensive and destructive burn events (Marlon et al., 2012; Willmore and Jensen, 1960). Such events have incurred millions of dollars in firefighting costs, as well as potential costs related to post-fire hydrologic and water quality concerns (Kulig et al., 2009).

Understanding the compound impacts of wildfires and climate change on hydrological processes and water quality constituents, such as organic carbon (OC), is crucial for informing effective land and water management decisions. The quantity and quality of source water supplies in many regions of the world are potentially vulnerable to catastrophic wildfire (Robinne et al., 2019) and climate change, and in most regions there is a lack of knowledge about physical and biogeochemical processes driving risks associated with these compounded events (Hallema et al., 2018; Robinne et al., 2019; Emelko et al., 2011). Some

* Corresponding author.
E-mail address: faramarz@ualberta.ca (M. Faramarzi).

https://doi.org/10.1016/j.jhydrol.2020.125403

Available online 13 August 2020

wildfires can affect hydrological processes by reducing canopy interception, decreasing evapotranspiration, and changing soil hydraulic properties, which results in decreased groundwater recharge, higher soil water content, greater peak flows and annual water yields (Ebel and Moody, 2017; Hallema et al., 2018; Townsend and Douglas, 2004). The loss of vegetation also exposes soils to forces exerted by precipitation, increasing the potential for erosion, sediment transport to streams, and debris flows (Gartner et al., 2008; Robichaud et al., 2016; Silins et al., 2009). Such effects can increase the delivery of water quality constituents, such as sediment and nutrients (i.e., OC, phosphorus, and nitrogen), to streams in both the dissolved (Rhoades et al., 2019) and particulate forms (Rust et al., 2018). For instance, suspended sediments (Cawley et al., 2018; Shakesby et al., 2015) and in-stream OC can increase following wildfires, and the dissolved fraction of OC is particularly challenging to remove from drinking water (Hohner et al., 2017). Organic carbon is a key water quality indicator due to its ability to transport heavy metals and organic contaminants, as well as support bacteria and biofilms (Fischer et al., 2002; Laudon et al., 2012). Often, high severity wildfires consume soil organic matter (Plaza-Álvarez et al., 2018; Smith et al., 2011), leaving mixed layers of ash (Smith et al., 2011) and other incomplete combustion products, such as charcoal and charred biomass, which contain OC in the form of pyrogenic carbon (PyC) (Abney et al., 2019). As well, alluvial deposits and increased suspended solid levels can facilitate dissolution of particulate organic matter attached to solid particles (Cawley et al., 2018; Cotrufo et al., 2016; Writer et al., 2012). However, the magnitude and longevity of effects to wildfire generally remain uncertain, especially if fires were to coincide with climate change.

A comprehensive representation of physical and biogeochemical processes (e.g., hydrologic and nutrient cycles and dynamics from terrestrial to water bodies) at the watershed scale is key for quantifying the impacts and reducing the potential risks associated with wildfires and climate change. Many researchers have applied hydrological models to assess watershed responses to climate change, land cover changes, disturbances, and extreme weather events, by analyzing relative changes in water quantity or quality parameters (Larsen et al., 2011; Malagó et al., 2017; Shrestha and Wang, 2018). Lumped, regression models may be useful in those rare instances when data is available both before and after discrete disturbance events, like wildfires (Rodríguez-Jeangros et al., 2018; Yu et al., 2019). However, even then, model application may be limited to establishing site-specific empirical relationships (e.g., Rodríguez-Jeangros et al., 2018; Yu et al., 2019), which lack representation of the dynamical biogeochemical processes and often fail to accurately predic the impacts. Therefore, it is often not possible to use such models to predict changes at the watershed scale under changing climate or land cover. Comparatively, physical process-based models have a distinct advantage in their applicability to develop and test “what if” scenarios to project expected changes in water quantity and quality to future climate change, extreme weather events, or discrete disturbance events such as wildfires. These models have been widely used in the past decade for simulation of erosion and in-stream sediment, nitrogen, and phosphorus (e.g., Malagó et al., 2017; Shrestha and Wang, 2018), but lacked adequate representation of OC processes. Moreover, the majority of existing models are capable of simulating either the cycling and dynamics of nutrients in the terrestrial environment (Son et al., 2019; Iravani et al., 2019) or in the aquatic environment (e.g., Lessels et al., 2015), but generally lack the ability to model connections between terrestrial and aquatic ecosystems at a watershed scale.

The Soil and Water Assessment Tool (SWAT) is a semi-distributed and process-based hydrologic and water quality model that is capable of simulating both landscape and in-stream processes related to hydrology, in addition to plant growth, and sediment and nutrient (i.e., nitrogen (N) and phosphorus (P)) cycling, loading, and transport (Arnold and Fohrer, 2005; Neitsch et al., 2011). As such, SWAT has been extensively used for water quantity or quality studies across watersheds (e.g., Azari et al., 2017; Faramarzi et al., 2009, 2017; Gassman et al., 2010; Havel et al., 2018; Hernandez et al., 2018; Krysanova and White, 2015; Morán-Tejeda et al., 2015; Rodrigues et al., 2019; Worku et al., 2017). However, the majority of these studies have addressed changes in hydrological processes, erosion (Dutta and Sen, 2018; Wu et al., 2018), sediment transport (Fabre et al., 2019), nitrogen and phosphorus transport and cycling due to climate change or land management practices (Kemanian et al., 2011; Moriasi et al., 2015), organic carbon (Jepsen et al., 2019; Ozturk et al., 2018), and stream temperature (Ficklin et al., 2012; Giles et al., 2019) without centering on the post-wildfire impacts on hydrologic and biogeochemical processes. Comparatively, there have been limited studies addressing the effects of discrete disturbance events, such as wildfires, on both water quantity and quality. Nonetheless, a considerable disconnection is perceived among these studies, since most of them are either centered on hydrological water quantity or water quality processes. Havel et al. (2018) used a SWAT model to simulate the hydrologic response to the 2012 High Park and Hewlett wildfires in Colorado, projecting increases in total annual runoff volumes and corresponding decreases in subsurface flow. In another study, Hernandez et al. (2018) used SWAT to provide evidence for a substantial increase in median annual streamflow in ten watersheds affected by wildfire in the Northern US Rocky Mountains, but did not evaluate water quality effects. Similarly, Rodrigues et al. (2019) found that larger prescribed burn simulations increased streamflow and considerably reduced aquifer storage in a tropical Brazilian watershed. Morán-Tejeda et al. (2015) combined climate change and land cover scenarios for a mountainous watershed in Spain, and found that overall water yield decreased from 2021 to 2050 compared to 1961–1990, particularly in spring and summer months. In general, the majority of model-based studies have projected increases in surface runoff and streamflow due to wildfire scenarios and decreases associated with reforestation scenarios.

Given the rapidly shifting wildfire and climate regimes in many regions along with the lack of modeling efforts attempting to project the range of likely hydrologic effects, the objectives of our study were to develop process-based hydrological models to assess the effects of wildfires, compounded with climate change, on catchment-scale water quantity and key water quality parameters (e.g., sediment, OC). In spite of a broad application of the SWAT hydrologic model for water quality simulations at a watershed scale, current OC modeling in SWAT lacks processes associated with OC fate and transport in the streams and water bodies, therefore, making it improper for a comprehensive terrestrial-in-stream water quality analysis. There are several recent studies with a focus to improve the capability of the standard SWAT model in OC simulation (Fabre et al., 2019; Jepsen et al., 2019; Kemanian et al., 2011). Zhang et al. (2013) revised the soil OC CENTURY model, initially developed by Parton and Rasmussen (1994), and incorporated it as a new module called SWAT-C. This module improved simulation of soil organic matter residue processes such as decomposition and land–atmosphere carbon exchanges, thereby expanding the applicability of the model to climate change, and carbon sequestration and emission studies only in the land phase and yet lacking the in-stream processes (Zhang et al., 2013). Given these limitations of models in simulating OC dynamics, Du et al. (2020) recently developed the SWAT Organic Carbon Simulation Module (SWAT-OCSM), which can successfully simulate OC transport by erosion and runoff, in-stream OC processes such as transformation and reaction, and OC loading at the watershed scale. Thus, we developed an improved modeling framework to assess watershed responses to climate change and potential wildfires, and identified key processes that may influence future water quantity and quality at a high spatial and temporal resolution. To achieve this goal, our specific objectives were to (1) simulate hydrologic processes that drive streamflow, sediment yield, and organic carbon using an enhanced SWAT model (i.e., SWAT-OCSM, Du et al., 2020) while considering spatiotemporal dynamics of both terrestrial (i.e., soil) and in-stream processes at a watershed scale; (2) examine impacts of future

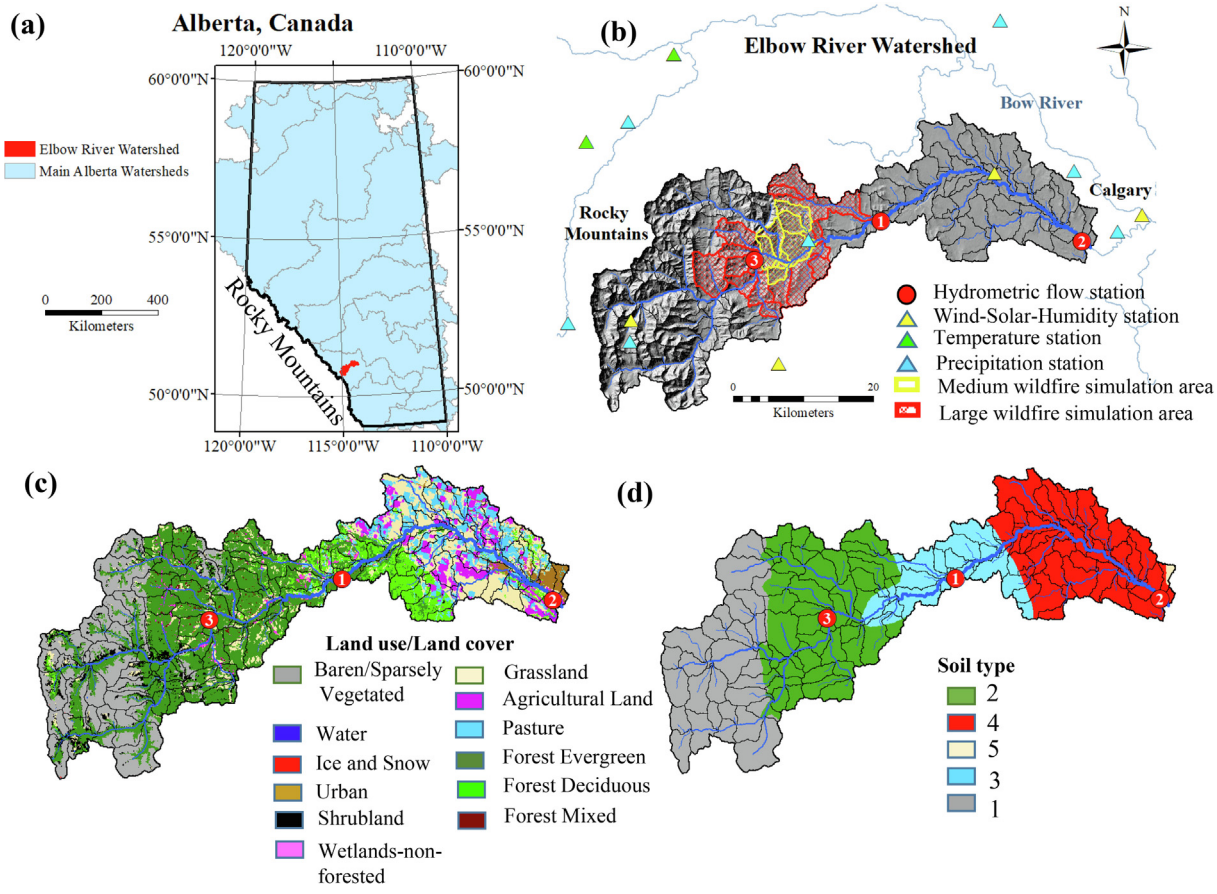

Fig. 1. (a) Location of Elbow River watershed in Alberta; (b) location of hydrometric stations (1. Bragg Creek; 2. Sarcee Bridge; 3. Elbow Falls) and climate stations. Areas for wildfire simulation are shown in yellow (6108 ha), and red (23,984 ha), based on local wildfire history (Rogeau et al., 2016); (c) land use/land cover distribution; (d) soil type distribution.

climate change scenarios, and simulate spatiotemporal variation of hydrological and water quality responses (i.e., sediment and OC); and (3) quantify long-term impacts of compounded wildfire and climate change on hydrologic processes as well as sediment and organic carbon loads and transport. To accomplish our objectives we focused our modeling efforts on the Elbow River (ER) watershed of southern Alberta, Canada. The ER watershed is characterized by heterogeneous soil, land use, and geospatial conditions, as well as cold region hydrology (e.g., Pomeroy et al., 2007) and has also been exposed to historical wildfires. Moreover, there was a unique long-term water quantity and quality dataset available in the study watershed, making it a suitable study area for model calibration and validation.

2. Materials and methods

2.1. Study area

The Elbow River (ER) is located in the montane and Rocky Mountain foothills region of southwest Alberta, Canada (Fig. 1). The headwaters originate in the mountains (3,205 m elevation) and flow east through boreal foothills forests (Fig. 1c). In the lower reaches of the watershed, the river flows through Aspen Parkland, which is flatter and has greater anthropogenic influence in the form of agriculture, pastures, and suburban residences. The lowest reach of our study area was the mouth of the Glenmore Reservoir (1,039 m elevation), which is the primary source of drinking water for 40% of the city of Calgary's 1.3 million people (Fig. 1b).

The regional climate is semi-arid with an average annual precipitation of 608 mm, with the Rocky Mountains (Fig. 1a) receiving approximately 750 mm of annual precipitation compared to approximately 350 mm in Calgary. The hydrology of the ER watershed is complex, as the watershed spans diverse landscapes where abrupt weather changes are common due to the influence of the Rocky Mountains (Fig. 1). Annual peak streamflow in the Elbow River generally occurs in June, coinciding with both peak snowmelt and spring rainfall. At Sarcee Bridge, near the watershed outlet, annual peak flows are approximately 30.1 m^3/s. Comparatively, the lowest flows (i.e., baseflow) occur in February each year at 2.2 m^3/s at Sarcee Bridge, which is primarily sourced from groundwater (Farjad et al., 2016). In the ER watershed, the distribution of vegetation is highly correlated with soil type (Fig. 1c, d), and details about soil properties are found in Table 1.

Wildfire is an important natural disturbance agent in the province of Alberta, influencing the structure of vegetation types within natural sub-regions (Cumming, 2001; Rogeau et al., 2016). The mean annual area burned in Alberta from 1961 to July of 2019 was 168,436 ha, with 10 of the 20 years with the highest burned area occurring since 2000 (Alberta Wildfire, 2019). Specific to our study, the Rocky Mountain region encompasses 7.4% of the area of Alberta, but has accounted for 12.6% of the annual area burned over the past ~ 60 years. Wildfires in the montane and foothills region previously occurred at intervals of approximately 26–39 years (Rogeau et al., 2016). Given that the last notable wildfire occurred in 1936, the region is statistically overdue for a large wildfire. The majority of other reported fires were either Class A (< 0.1 ha) or Class B (0.1–4.0 ha), and were primarily recreational or lightning-caused (Alberta Wildfire, 2019). In this study we tested impacts of lager potential fires as described in Section 2.4.2.

Table 1
Soil types, primary land uses, soil hydrologic group, and top layer composition. Note: rock refers to gravel; sand, silt and clay portions were normalized to 100%, and soil organic carbon is by weight.

Soil type	Land cover	Soil hydrologic group	Rock	Sand	Silt	Clay	Soil OC
1	Exposed rock with no vegetation - some evergreen forests in valleys	D: composed of solid rock with very low infiltration rates and low water transmission	–	–	–	–	–
2	Foothills or subalpine region - covered in evergreen forests	B: moderate infiltration rates, and moderately to moderately-well drained	2%	61%	17%	22%	7%
3	Mixture of evergreen and deciduous forest, with small urban land use in Bragg Creek	A: high water infiltration and transmission rates, and low runoff potential	15%	22%	60%	18%	30%
4	Agriculture, pasture, and grassland, with Calgary making up the easternmost portion	C: slow water infiltration and transmission rates, and high runoff potential	0	4%	54%	42%	4.8%

2.2. Hydrology and water quality simulation

The original release of the SWAT simulates both landscape and in-stream processes related to hydrology, plant growth, and sediment and nutrient cycling, loading, and transport. Subbasins within the model are further subdivided into hydrological response units (HRUs), within which all simulated processes occur homogeneously. Key hydrological variables simulated in the model are surface runoff, percolation, soil moisture, lateral flow, shallow groundwater recharge, evapotranspiration, and streamflow, among others (Neitsch et al., 2011). Water yield in SWAT is calculated as the sum of surface runoff, lateral flow, and groundwater flow contributing to streamflow in each subbasin, minus transmission losses through riverbed and pond storage (Neitsch et al., 2011).

The flow of water as surface runoff and through soils can impact water quality by transporting sediment and nutrients from hillslopes to streams. For sediments and nutrients (i.e., N and P), SWAT simulates erosion and deposition on the ground surface, as well as resuspension and deposition within streams. In the land phase simulation processes, nutrients (i.e., carbon (C), N and P) are closely interrelated through soil, microbial, and plant processes, including mineralization, immobilization, and humification (Neitsch et al., 2011). The rates of these reactions depend on factors such as soil temperature, soil moisture, clay content of soil, C:P and C:N ratios, as well as nutrient availability in the soil. Generally, carbon is added to soils through plant residue, and removed from soil via erosion and runoff. Because soil particulate organic carbon (POC) is primarily attached to finer clay particles that are more susceptible to erosion, the model calculates an OC enrichment ratio during storms and, therefore, the proportion of POC in surface runoff is typically higher than in the top soil layer.

To simulate in-stream processes associated with particulate and dissolved fractions of OC in the water column, and OC loading at the watershed scale, we used a recently developed SWAT-OCSM (Du et al., 2020) model. In this model, an in-stream OC simulation module is developed and embedded in the original SWAT model by modifying its source code, and the enhanced model is capable of simulating both terrestrial and in-stream processes. The improved model incorporates the SWAT-C module, developed by Zhang et al. (2013) for modeling soil organic matter processes, and simulates DOC and POC loadings entering the stream from surface runoff and erosion, as well as DOC transported by lateral flow and groundwater discharge to streams. The SWAT-OCSM also simulates in-stream reactions between OC, floating algae and streambed sediments, and instream transformations between POC, DOC, and inorganic carbon. A detailed description of SWAT-OCSM including formulae, parameters, and model testing are described in Du et al. (2020) and the processes are presented in Fig. A1. Model output data relevant to wildfire and climate change scenario analyses in this study include daily streamflow, sediment yield, and organic carbon yield at a HRU-to-subbasin spatial scale, which allowed us to investigate fluxes in water quantity and quality. Meanwhile, sediment and TOC yields are calculated as the total volume of sediment and TOC transported from land (i.e., HRU and subbasins) into the main channel, in addition to the total volume of sediment and TOC eroded from the stream bed and stream bank.

2.3. Model calibration and validation

Watershed delineation resulted in 154 subbasins (Fig. 1), which were further subdivided into 373 HRUs based on slope, land use type, and soil type. Monthly outputs were calibrated to measured streamflow, sediment yield, and organic carbon yield. The Nash-Sutcliffe Efficiency (NSE) was used as an objective function, and data from Bragg Creek and Sarcee Bridge stations were used for calibration (Du et al., 2020). The calibration period for streamflow was 2000–2015, and the validation period was 1986–1999, for which data from an additional station in the headwater region, Elbow Falls, was used for 1986–1995 (Fig. 1). The

model was further calibrated using sediment and TOC measurements at a daily time step. The calibration period was 2001–2007 and the validation period was 2008–2015 for both sediment and TOC loads (Du et al., 2020).

2.4. Scenario analysis

2.4.1. Simulation of climate change impacts

We applied the calibrated SWAT-OCSM model to assess changes in water quantity and quality under two climate scenarios in the near future (2015–2034) and the distant future (2043–2062). Streamflow, sediment yield, and TOC yields from the four scenarios were compared to historical simulations (1995–2014), which will herein be referred to the baseline period, in order to calculate relative changes. For our analysis, we considered the representative concentration pathways (RCP), including RCP 2.6 and RCP 8.5 for greenhouse gas emissions, as defined in the IPCC Fifth Assessment Report (2013). The RCP 2.6 projection is the optimistic case, in which global cooperation and cleaner technologies lead to reduced greenhouse gas emissions and CO_2 concentrations peak in mid-century. In the RCP 8.5 scenario, economic growth and emphasis on burning of fossil fuels lead to exponential growth in CO_2 concentrations throughout the century. Therefore, in this study we refer to RCP 2.6 as the best-case and to RCP 8.5 as the worst-case scenarios. For climate change simulations, CO_2 concentrations for near and distant future scenarios were 465 ppm and 485 ppm for RCP 2.6 and 485 ppm and 660 ppm for RCP 8.5, respectively. Average monthly temperature and precipitation for the historic period (1995–2014), the near future (2015–2034) and the distant future (2043–2062) are presented in Fig. 2.

For each of the four scenarios, we used climate projections of five general circulation models (GCMs) from Pacific Climate Impacts Consortium (PCIC) to address uncertainty associated with GCM projections (Table A1). The choice of the individual members of the ensemble was based on five GCMs that provide the widest spread in the projected future climate (Ammar et al., 2020). It is noteworthy that projected GCM data have been statistically downscaled to Canada (Cannon, 2015) and bias corrected to local climate conditions in Alberta (Masud et al., 2019; Ammar et al., 2020; Faramarzi et al., 2015). PCIC provides Canada-wide downscaled climate change projections using Bias-Correction Spatial Disaggregation (BCSD) and Bias Correction/Constructed Analogues with Quantile mapping reordering (BCCAQ) methods (http://www.pacificclimate.org/data). In our study, we used the projection derived using the BCCAQ method as it was evaluated by Werner and Cannon (2016) and was shown to pass the largest number of tests for hydrologic extremes in comparison to other methods including the BCSD using the ClimDEX indices recommended by the World Meteorological Organization Expert Team on Climate Change Detection and Indices (ETCCDI) (Chen et al., 2011). We further performed a secondary bias-correction of the PCIC data using the change factor method, i.e., the delta method (Chen et al., 2011) to reproduce historical streamflow in Alberta. Additionally, we tested the 0.9, 0.95, and 0.99 quantiles of the simulated streamflow for the historical period and the observed values were reproduced sufficiently by the hydrological model (Ammar et al., 2020). The future weather data was loaded into the calibrated SWAT-OCSM model, after which we investigated the impacts of climate change on water quantity and quality in subbasins and at the watershed outlet, Sarcee Bridge.

2.4.2. Simulation of the impacts of potential wildfire compounded with climate change

Wildfires of moderate and high burn severities were simulated for two areas (Fig. 1b), generating a total of four wildfire scenarios, which were combined with near future climate change scenarios (i.e., RCP 2.6 and RCP 8.5). Since a larger uncertainty is associated with distant future climate projections (IPCC, 2013), we have only tested our wildfire scenarios under near future climate change scenarios. Wildfire severity refers to the loss of biomass above or below ground (Keeley, 2009). Thus, low severity burns result in considerable tree survival and shallow burn depths within the soil, while high severity burns result in nearly all vegetation and root systems being incinerated. The smaller of the two areas for burn simulations included 6,108 ha in the west-central part of the watershed, intersecting the main stream (Fig. 1b). The larger wildfire simulation area was 23,984 ha, which included the entire small burn simulation area and more than half of the conifer forests of the upper ER watershed. This area is comparable to the 2003 Lost Creek wildfire that burned approximately 21,000 ha of high elevation forest in southwest Alberta (Silins et al., 2009). The wildfire scenarios will herein be referred to first by size, followed by burn severity: medium-moderate, medium–high, large-moderate, and large-high wildfire scenarios. Due to spatiotemporal dynamics of hydrological processes and water quality (e.g., Rust et al., 2018), we chose to simulate impacts of wildfires occurring on the 1st day of June for five years to allow for analysis of changes on a monthly basis, and for us to address inter-annual climate variability. We selected June for our analysis because most wildfires in the region occur in late spring. Additionally, based on historical climate data from Alberta Environment and Parks (Table A2), peak precipitation during this month, combined with late spring snowmelt, is likely to have the highest impact on water quality through erosion and OC loading.

We applied the wildfires scenarios in June as separate simulations to years 2026, 2027, 2028, 2030, and 2032, because future climate change data indicated lower precipitation in May in these years compared to

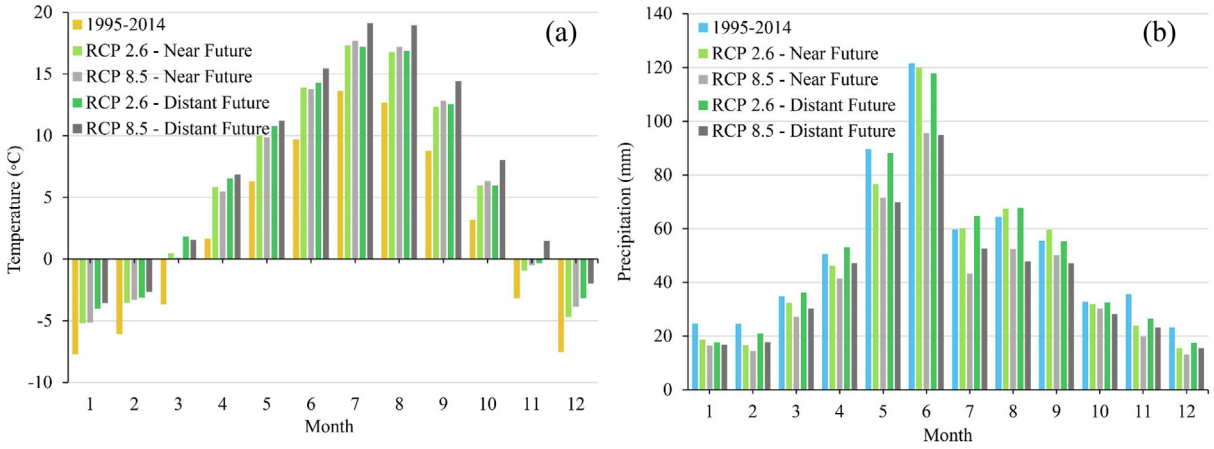

Fig. 2. Long-term average monthly precipitation (a) and temperature (b) for historical (1995–2014), near future (2015–2034) and distant future (2043–2062) periods averaged from the downscaled ensemble climate model data for RCP 2.6 and RCP 8.5 scenarios in this study.

Table 2
Default parameters used in SWAT-OCSM to simulate impacts of wildfire. The curve number (CN) is a default parameter defined in the land use database and varies according to soil type. CN is required for model initial run and it is updated on daily basis.

Parameter	Default Evergreen forest	Moderate burn severity Shrubland	High burn severity Grassland
CN for Soil type 2 (west-central)	55	61	69
CN for Soil type 3 (east-central)	25	39	49
Soil hydraulic conductivity (mm/hr)	300	250	200
Soil erodibility (USLE K)	0.15	0.25	0.35

other years, and dry conditions that would favor wildfire ignition. HRUs considered for wildfire simulations were chosen based on local wildfire history and elevation, as forests at lower elevations are hotter, drier, and thus more likely to burn (Rogeau et al., 2016). Therefore, we analyzed results of 200 individual wildfire simulations: 4 wildfire scenarios × 2 RCP climate change scenarios × 5 GCMs × 5 wildfires years = 200 total simulations.

To help parameterize our post-wildfire model we relied on published research on the effects of wildfires on hydrology and water quality (e.g., Ebel and Moody, 2017; Havel et al., 2018; Moody and Martin, 2009). To simulate post-wildfire conditions in SWAT-OCSM, we modified the code to change land use type and soil parameters in affected HRUs in the 'crop.dat' (Table 2) and 'basin.bsn' input files when a date was specified for a wildfire simulation, which is not feasible to modify within input data files and modification of the source code was necessary. The curve number is one of the most sensitive hydrologic parameters, and determines what proportion of rainfall infiltrates into the soil or becomes surface runoff (e.g., Gartner et al., 2008). In the model, default curve numbers are defined within land use parameters, and vary based on soil type. During SWAT simulations, curve numbers are updated on a daily basis based on soil permeability, land use type and vegetation growth, and initial soil water content from the previous day (Neitsch et al., 2011). To simulate the occurrence of wildfires in SWAT, we replaced evergreen forests in impacted HRUs with shrubs for moderate burn severity, and by grasses for high burn severity. The default curve numbers for shrubland are higher than those for evergreen forests, and higher yet for grassland (Table 2). Therefore, increases in curve numbers were reflective of burn severity, similar to Havel et al. (2018). For land use changes from evergreen forests to shrubland, the resulting curve numbers increased by 11% for soil type 2 (sandy clay loam) and 56% for soil type 3 (silt loam). For land use changes from evergreen forest to grassland in the case of severe wildfire simulations, the resulting curve numbers increased by 25% for soil type 2 and 96% for soil type 3. Similarly, research has shown that soil hydraulic conductivity (K_{sat}) often decreases with increasing burn severity (Ebel and Moody, 2017). We, therefore, reduced the K_{sat} in the model input data based on literature values (Table 2). It is important to note that our approach does not consider the potential temporary impact of a highly conductive ash layer, which often remains on the soil surface after a wildfire (Balfour et al., 2014). We also updated the soil erodibility parameter in SWAT (universal soil loss equation – USLE K) to reflect the typical increase in soil erosion that often occurs during the first years after wildfire (Table 2) (Moody and Martin, 2009).

Post-wildfire analysis involved assessing local changes in model outputs related to hydrology and water quality, including surface runoff, percolation, lateral flow, soil water content, evapotranspiration, sediment yield, and organic carbon yield in impacted subbasins. In addition, streamflow, in-stream sediment yield, and TOC yield were compared to those in non-wildfire simulations. With all wildfire simulations occurring on June 1st, we analyzed relative changes on a monthly basis from June–May in order to cover the 12-month period following the wildfire. It is noteworthy that in our simulations we only analyzed impacts on water quality-quantity for a year after each wildfire event, because it has been stated that wildfire impacts are most prominent in the first year or two years after. In addition, the hydrologic model is not designed to simulate post-wildfire vegetation succession.

Similar to climate change, we analyzed the relative changes due to wildfire at the watershed outlet, Sarcee Bridge; however, we also considered the Bragg Creek station due to its proximity to burned subbasins. As it was not possible to calibrate wildfire simulations due to the lack of measured data for post-wildfire periods, we assessed the performance of our simulations by comparing the scenario results with previous studies that have quantified the effects of wildfire on hydrology and water quality (e.g., Emelko et al., 2011; Havel et al., 2018; Silins et al., 2009).

3. Results and discussion

3.1. Model calibration and validation results

For streamflow calibration, the NSE was 0.62 for both Bragg Creek and Sarcee Bridge stations. The streamflow validation NSE was 0.62 for Elbow Falls, 0.75 for Bragg Creek, and 0.70 for Sarcee Bridge. For sediment load, the calibration NSE was 0.47 at Bragg Creek and 0.55 at Sarcee Bridge stations. The sediment load validation NSE was 0.21 at Bragg Creek and 0.13 at Sarcee Bridge. Our sediment results assessed as 'satisfactory' to 'very good' for calibration period, according to Moriasi's framework, and only in the validation period these results were not satisfactory but 'acceptable' according to the same study. The lower criteria efficiency that obtained for sediment load, as compared to streamflow, was partially attributed to limited observed sediment data for model evaluation that may not adequately reflect model performance for the study period. The limited availability of sediment data as compared to streamflow measurements is a common issue, therefore, some other literature suggests that NSE values for sediment simulation could be as low as 0.2 for a 'satisfactory' model performance (Tuppad et al., 2011; Ni and Parajuli, 2018). More specifically, the lower performance for the validation period as compared to calibration could be attributed to lower quality climate data for the validation period that were not available from the gauge stations in our watershed modeling (Du et al., 2020). The discrepancy in climate data caused an underestimation of peak flows and the resulting peak sediment loads, since limited precipitation and temperature data drew inadequate reflection of flood events due to rain or rain-over-snow processes. The Bagnold equation for in-stream sediment transport in SWAT (Neitsch et al., 2011) uses the stream power concept to simulate sediment deposition and re-suspension processes, which are very sensitive to peak flow simulation results. Therefore, incorporation of adequate climate data can considerably improve simulation of hydrological processes including sediment and therefore the validation results. However, these results do not affect our model performance, since model calibration results were more desirable. Moreover, our sediment simulations captured the order of magnitude of sediment loads with the PBIAS value less than 20% for the whole simulation period (i.e., both calibration and validation). The calibrated model was also able to capture seasonal and monthly variations according to the boxplots of observed and simulated sediment loads (see Fig. 6 in Du et al., 2020; and Fig. A2 in supplementary

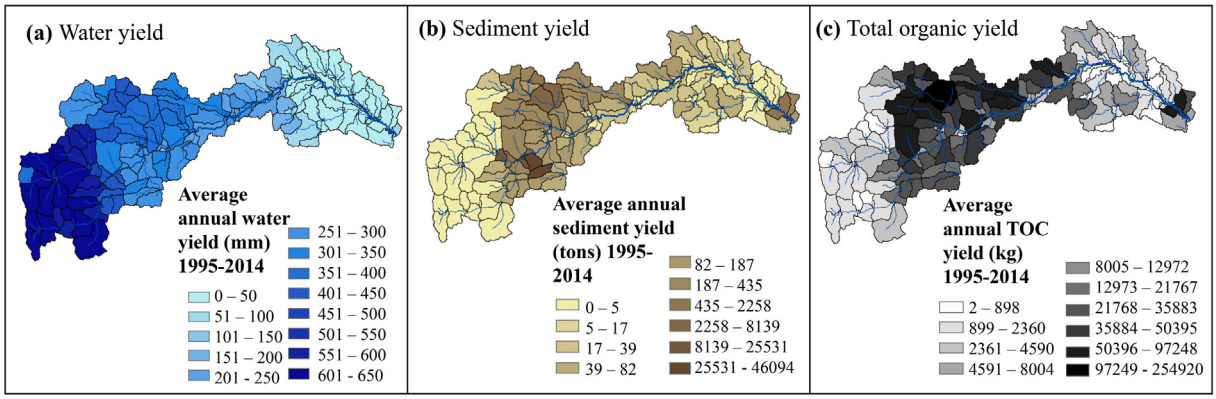

Fig. 3. Baseline conditions by subbasin for 1995–2014: (a) average annual water yield (mm); (b) average annual sediment yield (tons); (c) average annual TOC yield (kg).

material). Therefore, we used the calibrated sediment model to conduct scenario analysis as we focused on investigating the impacts on the changes in seasonal variations and in overall order of magnitudes, instead of predicting absolute changes in the future and under wildfire scenarios. For the TOC loads at Bragg Creek and Sarcee Bridge, the calibration NSE was 0.71 and 0.74, respectively, and the validation NSE was 0.57 and 0.66, respectively. All data sources are listed in Table A2, and example calibration results from Du et al. (2020) are presented in Fig. A3.

3.2. Spatial analysis of water, sediment, and TOC yields for the baseline period

Our SWAT-OCSM simulation results for the baseline period (1995–2014) demonstrated a similar spatiotemporal pattern for water yield, sediment yield, and total organic carbon (TOC) yields (Figs. 3 and 4), which is mainly because of the strong relation between hydrological processes and transport of sediment and TOC (e.g., Rostami et al., 2018). Spatially, water, sediment, and TOC yields by subbasin generally decreased moving from upstream to downstream subbasins during the baseline period (Fig. 3). Temporally, periods of low runoff in the winter consistently had the lowest sediment and TOC yields, whereas peak runoff in June corresponded to highest sediment and TOC yields (Fig. 4). On average, the uppermost subbasins draining into the Elbow Falls gauging station yielded 480 mm of water annually, and those between Elbow Falls and Bragg Creek yielded 310 mm of water, compared to only 84 mm in lower reaches between Bragg Creek and Sarcee Bridge (Fig. 3a). The west-to-east gradient was unsurprising, as there is nearly twice as much precipitation and the headwater catchments are steeper and more conducive to runoff generation in the Rocky Mountains relative to the eastern portion of the ER watershed.

Average sediment yield by subbasin for the baseline period generally followed water yield patterns, decreasing from west to east (Fig. 3b). However, the westernmost alpine region is composed primarily of bare, exposed bedrock (soil type 1, Table 1) and, as such typically yielded less than five tons of sediment per subbasin annually, despite receiving the most precipitation and having the steepest slopes and therefore, highest potential for runoff. (Fig. 1d; Table 1). While the bedrock is mildly erodible, the Rocky Mountain Front Ranges are generally underlain by more resistant lithology than the downstream Foothills (Osborn et al., 2006). As such, our model treated these regions as relatively resistant, resulting in sediment yields that predominantly originated from channel and bank erosion processes. The mid-upper sub- watershed generated the highest sediment yields, with an average of 3,317 tons per subbasin annually. The subbasins in this portion of the ER watershed generally have a sandy clay loam (soil type 2) top soil, which supports predominantly conifer forests. Interestingly, the two major subwatersheds downstream of the highest sediment yielding subcatchment, only generated ~1.0% (33 tons per subbasin annually) and ~0.4% (12 tons per subbasin annually) of the sediment yields. These lower portions of the ER watershed generally receive the lowest annual precipitation, have gentler hillslopes, are dominated by silt loam (soil type 3) or silty-clay (soil type 4) soils, and support mixed land use with agriculture, pastureland, grassland, and some deciduous dominated forests. Not surprisingly, annual sediment yields rose to 464 tons per subbasin near the watershed outlet in the subbasins dominated by urban development. This is consistent with many studies that have illustrated the strong influence of urbanization and associated impervious surfaces on delivery of suspended sediment to streams (e.g., Chen and Chang, 2019; Meierdiercks, et al., 2010).

Spatial distribution of TOC yield by subbasin was comparable to that of sediments (Fig. 3c). An average of only 2,834 kg of OC originated from the western subbasins with soil type 1 annually, as the model input data had no initial soil OC content for the exposed bedrock (Fig. 1d; Table 1). Therefore, the primary sources of TOC were channel and bank erosion. Additional sources of TOC included DOC transported by surface runoff, lateral flow, debris from terrestrial and aquatic vegetation, and in-stream processes such as dissolution of POC. Similar to sediment, the mid-upper (soil type 2, sandy clay loam soils) and mid-lower (soil type 3, silt loam soils) subbasins generated the highest amounts of TOC annually at 38,739 kg and 26,082 kg, respectively. This is partially attributable to the initial soil OC content, which was 7% in the sandy clay loam soils of the mid-upper subbasins and 30% in the silt loam soils of the mid-lower subbasins. The greater relative contribution of TOC to the streams in these subbasins was likely related to the annual regeneration of soil OC through forest plant litter and the steeper slopes in these subbasins, which can accelerate runoff and erosional processes. In comparison, the eastern subbasins, which were dominated by agricultural land, generated an average of only 2,391 kg of TOC annually by subbasin due to lower initial soil OC content of 4.5%, as well as gentler slopes and less precipitation compared to the central areas. The urban areas near the watershed outlet yielded 33,336 kg of TOC.

3.3. Analysis of the impacts of climate change

3.3.1. Streamflow

Streamflow at the ER watershed outlet, Sarcee Bridge, decreased in both the near future (2015–2034) and distant future (2043–2062) models, compared to the baseline period (1995–2014) (Fig. 4a; Table 3). Reduced streamflow was most prominent in the summer months of June, July, and August, which was related to lower summer rainfall and hotter temperatures that accelerate evapotranspiration (Fig. 2). This is consistent with previous observations of considerable reductions in summer streamflow in several Rocky Mountain streams, which have been attributed to warming temperatures and earlier onset

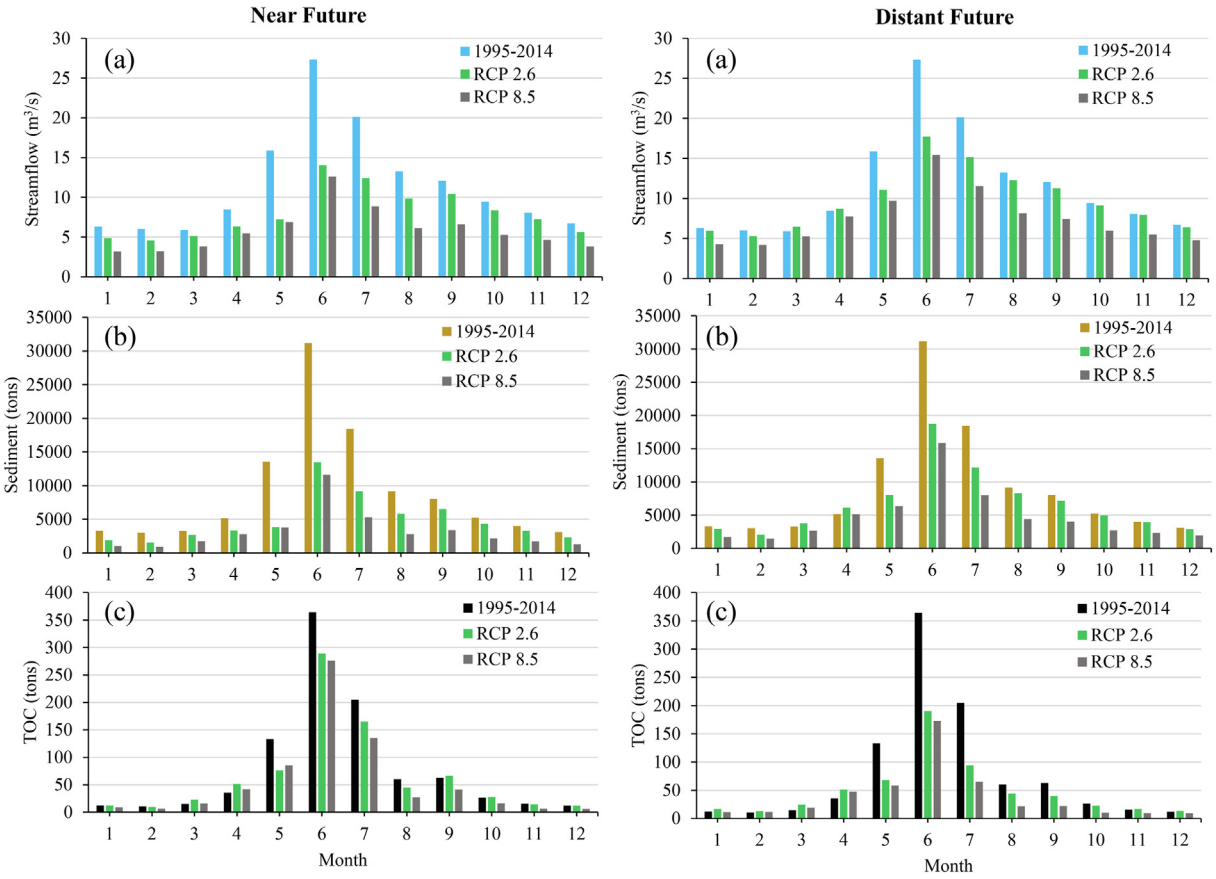

Fig. 4. Long-term monthly averages (January to December) for historical (1995–2014), near future (2015–2034) and distant future (2043–2062) periods at Sarcee Bridge station near watershed outlet: (a) streamflow (m^3/s); (b) sediment yield (tons); (c) organic carbon yield (tons).

of snowmelt (Rood et al., 2008; Leppi et al., 2012). Not surprisingly, in our study, the RCP 8.5 scenario projected lower streamflow than the RCP 2.6 scenario for each month, with the largest relative differences in July–November. This was anticipated, as the RCP 2.6 scenario has projected higher precipitation and lower overall temperature than the RCP 8.5 scenario.

Decreases in annual streamflow relative to the baseline period were greater during the near future scenario compared to the distant future scenario. In the near future model runs, annual streamflow decreased by 25% and 47% for RCP 2.6 and RCP 8.5 scenarios, respectively. Comparatively, in the distant future model runs, annual streamflow decreased by only 10% and 32% for RCP 2.6 and RCP 8.5 scenarios, respectively (Table 3). We attribute the higher streamflow in the distant future period for both scenarios to a slight increase in precipitation relative to the near future (Fig. 2) (Masud et al., 2018; Ammar et al., 2020). However, hotter temperatures in the distant future would lead to higher evapotranspiration rates. Given that we did not observe this outcome, we hypothesized that plants had greater water use efficiency because of higher atmospheric CO_2 levels in the distant future, thereby decreasing transpiration rates (Monteith, 1965; Deryng et al., 2016), resulting in smaller declines in streamflow than expected simply by considering potential evapotranspiration. The trends observed in our analysis are consistent with another study of the ER watershed, for which climate change scenario results of a physical process-based model, MIKE SHE/MIKE 11, suggested higher streamflow in the 2050′s relative to the 2020′s (Farjad et al., 2016).

3.3.2. Sediment yields

Model results suggested that changes in future sediment yields at the ER watershed outlet may exhibit similar trends to streamflow for both RCP scenarios, reinforcing the strong relationship between streamflow and erosion (Fig. 4b; Table 3). In the near future scenarios (2015–2034), annual sediment yields decreased by 37% for the RCP 2.6 scenario and 62% for the RCP 8.5 scenario. Comparatively, in the distant future scenarios (2043–2062), sediment yields only decreased 13% for the RCP 2.6 scenario and 42% for the RCP 8.5 scenario. These results suggested that, on average, water entering the Glenmore Reservoir would have lower total suspended solids (TSS) concentrations compared to the present day period. However, erosion patterns were projected to change heterogeneously within the ER watershed and little difference was observed between the RCP 2.6 and RCP 8.5 scenarios (Fig. 5). In the near future, central subbasins sandy clay loam soils (type 2) were projected to undergo significantly less erosion despite yielding the most sediments during the baseline period (Fig. 3b). Conversely, both scenarios in the distant future projected sediment yield increases of > 500% for the same region (Fig. 5), which is likely due to overall higher precipitation compared to the near future, and intensified rainfall and flood events (Ammar et al., 2020). In the distant future RCP 2.6 scenario, precipitation is considerably higher than for RCP 8.5 (Fig. 2), but a higher CO_2 concentration in RCP 8.5 can offset the impacts of lower precipitation as plants will transpire less water due to CO_2 saturation (Deryng et al., 2016). In such a scenario, this would result in additional water available for runoff, and therefore similar spatial sediment yield patterns between RCP 2.6 and RCP 8.5 scenarios (Fig. 5). Furthermore, lower water demand by plants due to elevated CO_2 levels may leave more water available for streamflow and thus stream bed and bank erosion (Deryng et al., 2016; Keenan et al., 2013). Although remarkable, these erosion increases in the distant future were not reflected at the watershed outlet, indicating that sediment deposition was a dominant process within the channel due to lower streamflow power. However, higher erosion rates increased sediment available for transport during storms through resuspension, which can cause higher

Table 3
Climate change scenario results for Sarcee Bridge at watershed outlet: % change in streamflow, sediment yield and TOC yield, relative to baseline period (1995–2014): (a) near future; (b) distant future. Note: winter TOC yields are very low between October-March for baseline period.

(a) Near Future (2015–2034)

Month	Streamflow			Sediment Yield			TOC Yield		
	Baseline (m^3/s)	RCP 2.6	RCP 8.5	Baseline (tons)	RCP 2.6	RCP 8.5	Baseline (tons)	RCP 2.6	RCP 8.5
Jan	6.3	−23%	−50%	3300	−42%	−68%	12.2	−1%	−28%
Feb	6.0	−24%	−47%	3000	−49%	−70%	10.8	−12%	−40%
Mar	5.9	−13%	−35%	3300	−18%	−48%	14.8	54%	7%
Apr	8.5	−25%	−35%	5100	−35%	−46%	35.5	45%	18%
May	15.9	−55%	−57%	14,000	−72%	−72%	133.4	−43%	−36%
Jun	27.3	−49%	−54%	31,000	−57%	−63%	364.4	−21%	−24%
Jul	20.1	−38%	−56%	18,000	−50%	−71%	205.0	−20%	−34%
Aug	13.2	−26%	−54%	9100	−36%	−70%	60.2	−25%	−55%
Sep	12.1	−14%	−45%	8000	−19%	−58%	62.9	6%	−34%
Oct	9.4	−11%	−44%	5200	−17%	−59%	26.4	6%	−39%
Nov	8.1	−10%	−43%	4000	−17%	−57%	15.4	−6%	−57%
Dec	6.7	−16%	−43%	3100	−26%	−58%	11.9	−3%	−50%
Average	11.6	−25%	−47%	9000	−37%	−62%	79.4	−2%	−31%

(b) Distant Future (2043–2062)

Month	Streamflow			Sediment Yield			TOC Yield		
	Baseline (m^3/s)	RCP 2.6	RCP 8.5	Baseline (tons)	RCP 2.6	RCP 8.5	Baseline (tons)	RCP 2.6	RCP 8.5
Jan	6.3	−6%	−32%	3300	−11%	−49%	12.2	38%	−6%
Feb	6.0	−12%	−30%	3000	−31%	−51%	10.8	21%	7%
Mar	5.9	10%	−11%	3300	15%	−18%	14.8	66%	27%
Apr	8.5	3%	−8%	5100	20%	0%	35.5	45%	34%
May	15.9	−30%	−39%	14,000	−41%	−53%	133.4	−49%	−56%
Jun	27.3	−35%	−44%	31,000	−40%	−49%	364.4	−48%	−53%
Jul	20.1	−25%	−43%	18,000	−34%	−57%	205.0	−54%	−68%
Aug	13.2	−7%	−39%	9100	−9%	−52%	60.2	−27%	−64%
Sep	12.1	−7%	−38%	8000	−11%	−50%	62.9	−37%	−65%
Oct	9.4	−3%	−37%	5200	−5%	−48%	26.4	−15%	−61%
Nov	8.1	−1%	−32%	4000	−2%	−41%	15.4	9%	−39%
Dec	6.7	−5%	−29%	3100	−7%	−38%	11.9	12%	−24%
Average	11.6	−10%	−32%	9000	−13%	−42%	79.4	−3%	−31%

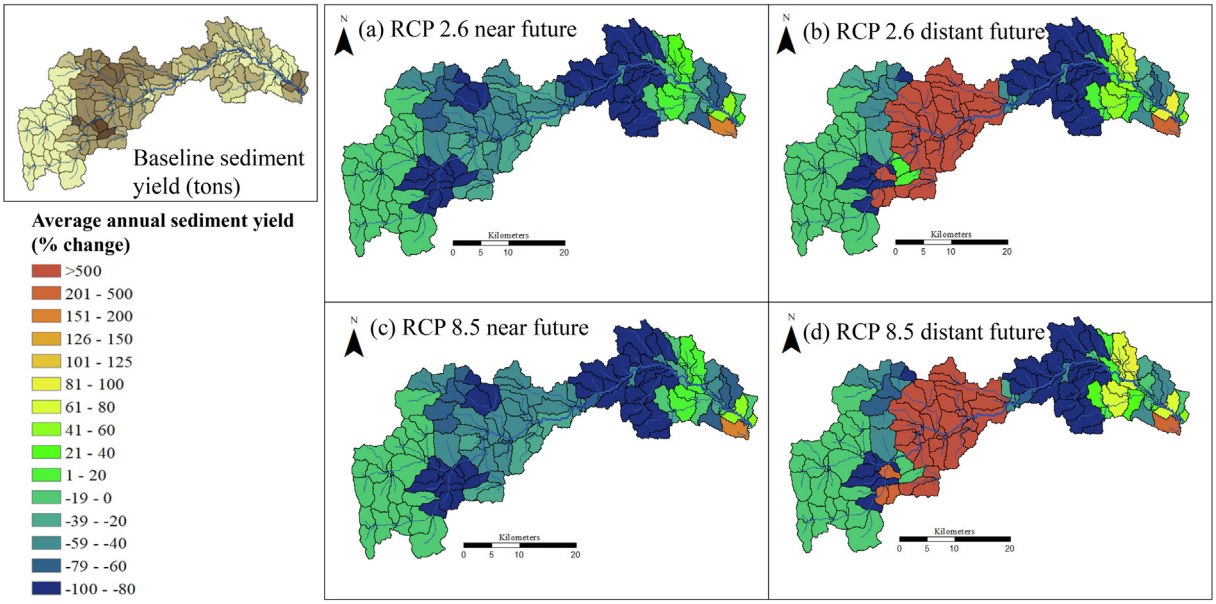

Fig. 5. Relative changes in sediment yield (% change) compared to baseline period (1995–2014) in Fig. 3b: (a) RCP 2.6 near future (2015–2034); (b) RCP 2.6 distant future (2043–2062); (c) RCP 8.5 near future (2015–2034); (d) RCP 8.5 distant future (2043–2062).

sediment fluxes for individual events. It is notable that analyzing 20-year averages did not address effects of individual extreme rainfall events, during which sediment loads entering the Glenmore Reservoir may have sharp peaks lasting a few days. This is mainly because our model underestimated peak flows and the resulting peak sediment loads as described in Section 3.1.

3.3.3. Organic carbon yields

Average annual TOC yields declined under both climate change scenarios, but patterns diverged from those of streamflow and sediment yield (Fig. 4c and Table 3). Similar to streamflow and sediment yield trends, the largest relative decreases in TOC yield occurred in the late spring and summer months. Annual TOC yields decreased by 2% and 3% in the near and distant future of the RCP 2.6 scenario, respectively, compared to the baseline period. Since streamflow decreased with larger relative rates (e.g., by 25% and 10%) for the same periods, a poorer water quality was expected in both future periods, particularly in the near future, due to higher suspended POC and higher DOC concentrations (see detailed explanation later in this paragraph). Likewise, the RCP 8.5 scenario results suggested poorer overall water quality in terms of OC compared to the baseline period, particularly in the near future. Overall, a key difference between TOC and projected streamflow and sediment trends is that TOC yield was higher in the near future compared to the distant future in the watershed outlet. Relative changes in spatial TOC yields, however, do not explain such divergence because they were similar to those of sediment yields, with near future TOC yields decreasing in central mountain subbasins, compared to large relative increases in the distant future (Fig. 6). Moreover, eastern agricultural subbasins with silty clay soils (type 4) revealed higher TOC yields, which were more pronounced in the distant future. While it is understood that surface runoff and erosion are important export mechanisms for TOC (e.g., Rostami et al., 2018), the fact that relative decreases in sediment yields are more pronounced than those for TOC yields (see Figs. 4–6), suggests that additional processes related to OC are simulated and play an important role. These processes in our SWAT-OCSM model include DOC transport to the main stream via surface runoff, lateral flow and groundwater flow, in-stream transformations, as well as growth and settling rates of floating algae (Du et al., 2020). Algae growth rates are a function of temperature (e.g., Nalley et al., 2018), and therefore are likely to increase due to climate change, contributing to higher in-stream POC, in addition to higher contributions from landscape erosion. The POC can then remain in suspension, settle to the bed sediment, or dissolve into DOC. Increased in-stream erosion can also facilitate the dissolution of organic matter attached to the sediment particles (Cawley et al., 2018). Furthermore, in-stream reaction rates of POC and DOC in SWAT-OCSM accelerate in warmer waters, and water temperature is calculated based on air temperature. Therefore, we hypothesized that in the near future, higher temperatures would lead to faster POC dissolution rates to DOC, and a significantly lower summer streamflow would lead to higher concentrations of OC. Winter months, under the RCP 2.6 scenario, typically revealed elevated TOC yields relative to baseline conditions as compared to the RCP 8.5 scenario. This is likely because higher streamflow in RCP 2.6 could transport more POC, which dissolves to DOC and is more easily transported to the watershed outlet (Fig. 4). As for the distant future scenarios, higher temperature relative to the near future (Fig. 2) could even further accelerate POC dissolution to DOC, and subsequently accelerate the rate of DOC mineralization, effectively decreasing the organic fraction of carbon and thus TOC export.

3.4. Impacts of potential wildfire compounded with climate change

3.4.1. Local changes

Here we report the results of the potential wildfire impacts compounded with climate change by explaining changes in hydrological processes (i.e., surface runoff, percolation, lateral flow, soil water, and evapotranspiration), and consequently the water quality constituents such as sediment yields and OC during the first year after the wildfire event. We illustrate projected magnitudes under climate change only in Fig. 7, columns a and d, and the corresponding range of parameter values for subbasins within the wildfire perimeter are presented in Table 4. The anomalies of 'climate change compounded with wildfire' from 'climate change only' scenarios are illustrated in Fig. 7, columns b,c,e,f, and the range of percentages are provided in Table 4. It should be noted that, only relative changes in wildfire-impacted subbasins for the large area (23,984 ha) scenarios, i.e., moderate and severe burns, are presented; the medium area (6,108 ha) scenarios are not shown, because they are encompassed by the large area, and relative changes by subbasin were identical to those in the large area scenarios (see Fig. 1b).

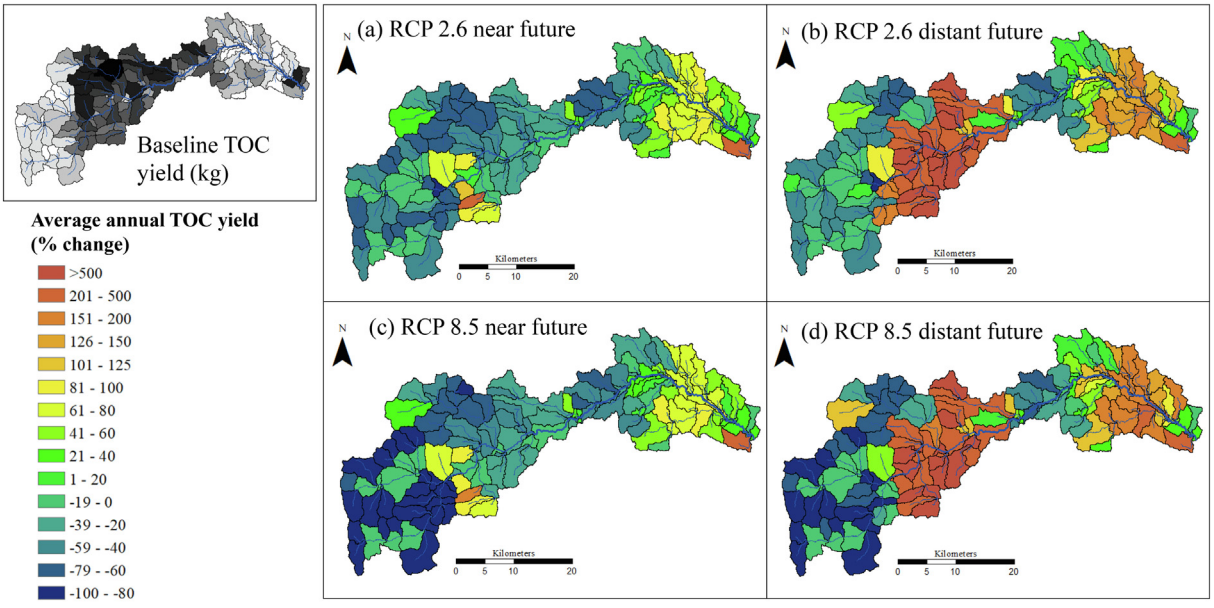

Fig. 6. Relative changes in TOC yield (% change) compared to baseline period in Fig. 3c: (a) RCP 2.6 near future (2015–2034); (b) RCP 2.6 distant future (2043–2062); (c) RCP 8.5 near future (2015–2034); (d) RCP 8.5 distant future (2043–2062).

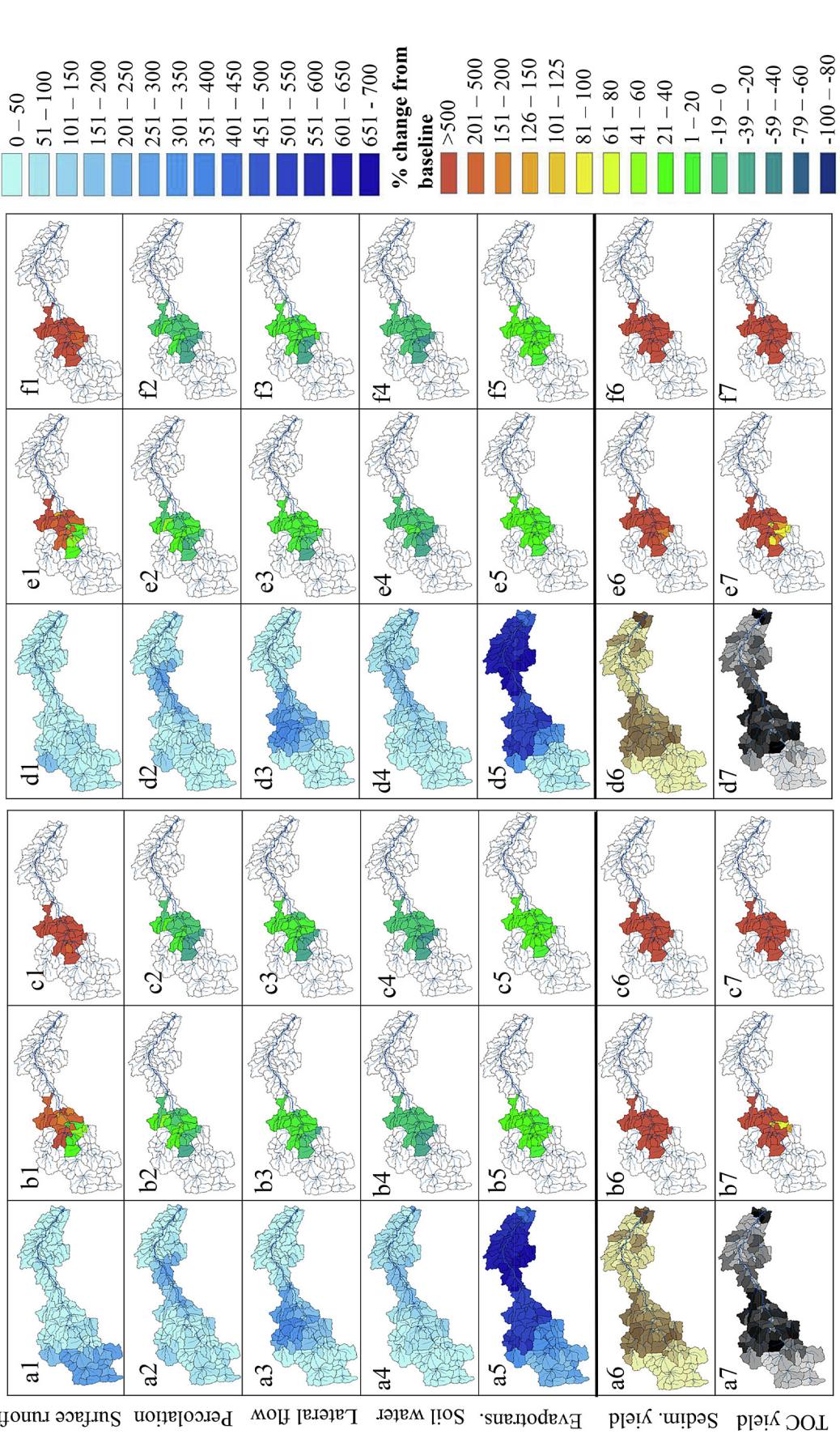

Fig. 7. Relative changes in post-wildfire hydrological processes (surface runoff, percolation, lateral flow, soil water, and evapotranspiration) and water quality parameters (sediment yield and total organic carbon yields) for large burn area one year after wildfire – average of wildfire simulations in years 2026, 2027, 2028, 2030, and 2032. All anomalies are calculated as: [projected data under wildfire compounded with climate change]/[projected data under climate change only] × 100. Note: relative changes in medium area scenarios (not shown) are identical for impacted subbasins; burn perimeter is presented in Fig. 1b; initial values and relative changes (%) presented in Table 4.

Table 4
Initial range of parameters for 'climate change only' scenarios in subbasins within wildfire perimeter, and relative changes one year after wildfire – average of wildfire simulations in years 2026, 2027, 2028, 2030, and 2032. All anomalies are calculated as: [projected data under wildfire compounded with climate change-projected data under climate change only]/[projected data under climate change only] × 100. Note: relative changes in medium area scenarios (not shown) are identical for impacted subbasins; large burn area is shown in Fig. 1b; spatial distribution of parameters in Fig. 7.

RCP 2.6			
	Without Wildfire	Moderate Severity Anomalies	High Severity Anomalies
Surface Runoff	26 to 94 mm	11% to > 500%	417% to > 500%
Percolation	13 to 276 mm	−22% to 55%	−32% to 28%
Lateral Flow	80 to 360 mm	−21% to 16%	−26% to 10%
Soil Water	43 to 153 mm	−33% to −1%	−42% to −6%
Evapotranspiration	319 to 567 mm	11% to 40%	11% to 39%
Sediment Yield	7.1E-04 to 209.5 ton	> 500%	> 500%
TOC Yield	1.6 to 1.4E+05 kg	76% to > 500%	227% to > 500%
RCP 8.5			
	Without Wildfire	Moderate Severity Anomalies	High Severity Anomalies
Surface Runoff	25 to 95 mm	17% to > 500%	211% to > 500%
Percolation	12 to 277 mm	−21% to 40%	−29% to 11%
Lateral Flow	80 to 363 mm	−20% to 20%	−26% to 21%
Soil Water	42 to 153 mm	−32% to 1%	−40% to −5%
Evapotranspiration	318 to 561 mm	11% to 39%	11% to 39%
Sediment Yield	16.2E-04 to 212.9 ton	174% to > 500%	> 500%
TOC Yield	1.4 to 1.4E+05 kg	85% to > 500%	392% to > 500%

The results of our model indicated that wildfires could increase subbasin annual surface runoff by 11% to > 500%, with annual increases ranging between 2 and 55 mm by subbasin (Fig. 7a1–f1; Table 4). Increased surface runoff is related to the increase in curve number associated with land cover changes, in addition to reduced soil hydraulic conductivity due to fire that resulted in lower soil water content and greater water availability for surface runoff (e.g., Ebel and Moody, 2017). Our results are consistent with several empirical studies of wildfire effects on annual water yields. For example, Mahat et al. (2016) observed mean annual water yield increases of 19–101% across the first five years after wildfire in two watersheds in the Canadian Rocky Mountains. Comparatively, others have reported increases in runoff and annual water yields of 16–200% during the first several years after wildfire (Bart, 2016; Wine and Cadol, 2016; Niemeyer et al., 2020). We posit that the large increases in runoff from our high severity model scenarios provide insights into the potential magnitude of effects due to shifting wildfire regimes towards increasingly high severity combined with increases in potential evapotranspiration associated with climate change. Similar to our study, Havel et al. (2018) also modeled post-wildfire hydrological changes using SWAT based on measured streamflow in a Colorado watershed, and determined that annual surface runoff in wildfire-impacted subbasins increased between 40 and 51 mm. However, the greatest observed increase was approximately 75% in subbasins with high burn severities in their watershed, compared with over 500% for the ER watershed model. The seemingly large variance between the two findings is likely due to differing hydrogeological conditions. For example, the ER watershed had very low surface runoff in simulations of climate change impacts without wildfires (Fig. 7a1,d1; Table 4) and a small change due to wildfire resulted in a large anomaly. In addition, curve numbers in the ER watershed model were increased by 11–56% and 25–96% for moderate and high burn severities, respectively, and varied between the two soil types, compared to only 10% and 15% in the Colorado study, respectively. However, it is also important to note that Havel et al. (2018) based spatial land use changes on satellite imagery, and calibrated curve numbers in their model to hydrometric station data that were available for the pre-wildfire and post-wildfire periods. They also did not directly measure surface runoff in the field, nor modify soil hydraulic conductivity, which can also impact runoff (Ebel and Moody, 2017). In comparison, curve numbers for post-wildfire simulations in our model of the ER watershed were initially obtained from the land use database for the grass and shrub land use inputs that were already present in the ER watershed model in locations outside the wildfire boundary and they were updated in the model on a daily basis (see Section 2.4.2 and Fig. 1c).

Impacts on annual percolation in the ER watershed were also variable within the wildfire boundary, generally decreasing in impacted subbasins but also increasing in some subbasins (Fig. 7a2–f2; Table 4). This confirms the important role of forests in regulating water quantity through prevention of instantaneous surface runoff, resulting in more water available for infiltration and percolation (e.g., Moody and Martin, 2001; Townsend and Douglas, 2004). Simulation of percolation in SWAT is a function of existing soil water content, soil water storage capacity, and plant water uptake among other parameters. Therefore, it is conceivable that water available for percolation and soil saturation increased slightly in some subbasins due to mortality of trees and the consequent reduction of interception and plant transpiration, in spite of lower hydraulic conductivity and higher curve numbers (Table 2) (Neitsch et al., 2011).

In the ER watershed model, the spatial changes in lateral flow generally followed percolation patterns by increasing in some affected subbasins, while decreasing in others (Fig. 7a3–f3; Table 4). However, a higher proportion of wildfire-impacted subbasins exhibited increases in lateral flow, whereas a higher proportion of subbasins exhibited decreases in percolation. In our hydrologic model, lateral flow occurred when an impermeable layer (i.e., a layer with very low hydraulic conductivity) existed in deeper soil layers and when soil water saturation above that layer reached a certain threshold in the model. The volume of moisture in the soil and whether it reaches saturation depends on the portion of infiltrated water that vegetation roots uptake from the soil, which in turn is based on the daily growth of plant biomass. The available water capacity of soil, and soil types and their hydraulic conductivities among other properties in the root zone impact daily growth rate of plant biomass. Therefore the occurrence of lateral flow is generally not simple but results from collective processes making up the overall soil water balance. This confirms the complexity of interactions between curve numbers, water uptake by plants, soil properties such as water capacity and K_{sat}, water infiltration, among other hydrological processes. Given the importance of lateral flow for streamflow in many catchments, and the difficulty of quantifying these subsurface processes (James and Roulet, 2007), our modeled outputs provide valuable projections of what might be expected under various future wildfire and climate change scenarios. Our results are consistent with others who have observed ~15–25% decreases in lateral flow after wildfire due to reduced infiltration and evapotranspiration (Jung et al., 2009).

Post-wildfire soil water content also decreased in most subbasins due to higher proportions of water lost by surface runoff. (Fig. 7a4–f4; Table 4). This was an interesting result of the model and similar to observations after the Fourmile Canyon wildfire in the Colorado Front Range of the Rocky Mountains that showed reduced post-fire soil water content responses to storm events due to decreased infiltration below the ash layer and increased surface runoff (Ebel and Moody, 2017).

In part, the post-fire decrease in soil water content may also be attributed to the higher rates of evapotranspiration in the burned watershed, as produced by our model. Our model results showed similar magnitudes of change for the two RCP scenarios, with increases in ET

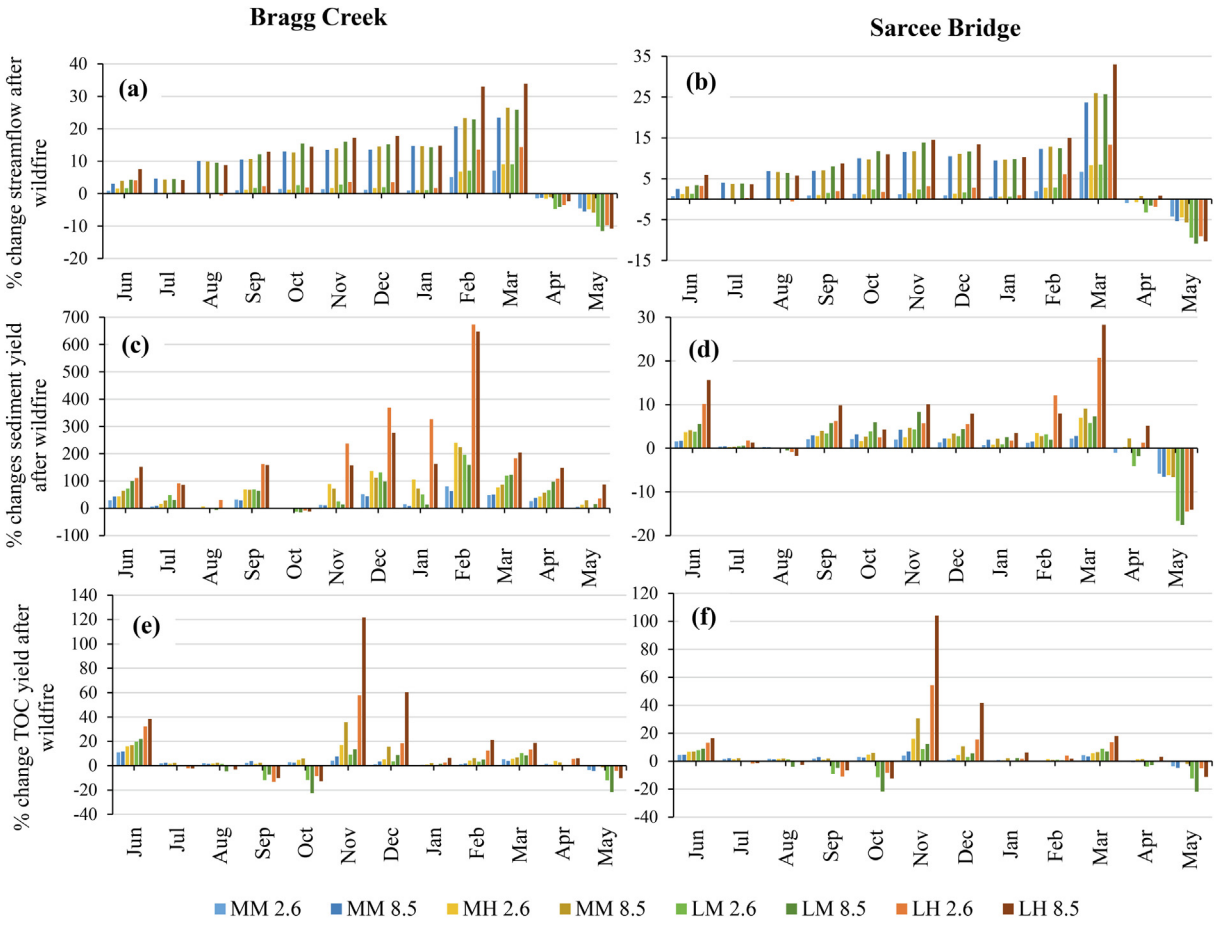

Fig. 8. Relative changes in streamflow, sediment yield and TOC due to wildfires at Bragg Creek station and Sarcee Bridge station at watershed outlet. All results are the average from wildfire simulations in the years 2026, 2027, 2028, 2030, and 2032. MM = medium area, moderate burn severity; MH = medium area, high burn severity; LM = large area, moderate burn severity; LH = large area, high burn severity.

between 11 and 39% (Fig. 7a5–f5). In the moderate burn severity scenarios, evapotranspiration increased between 24 and 68 mm annually for the RCP 2.6 scenario (Fig. 7b5), and between 21 and 62 mm for the RCP 8.5 scenario (Fig. 7e5). For the high severity, burn scenarios, evapotranspiration increased between 23 and 70 mm by subbasin for the RCP 2.6 scenario (Fig. 7c5), and between 21 and 70 mm for the RCP 8.5 scenario (Fig. 7f5). This was somewhat surprising as empirical research has illustrated ~15–45% lower evapotranspiration in catchments burned at moderate to high severity (Poon and Kinoshita, 2018; Blount et al., 2019; Niemeyer et al., 2020). However, to model the wildfire scenarios conifer forests were converted to grasslands in our ER study. While some studies have generally noted higher ET rates from conifers forests (Bosch and Hewlett, 1982; Newson, 1985; Kirby et al., 1991; Hudson et al., 1997), there have been observations of higher ET in grass dominated systems (Kelliher et al., 1993; Liu et al., 2003). These conflicting results from earlier studies is likely because the higher total evapotranspiration on a yearly average in forests is attributed to the higher rates of evaporation from canopy storage, i.e., interception evaporation, but not transpiration, and their transpiration is significantly smaller than other landuse types such as grasslands (Robinson and Dupeyrat, 2005; MirHadi Madani et al., 2018). In addition, total evapotranspiration from forests depends on tree types (e.g., coniferous versus broad leaf) and their canopy structure, phenology, and stomatal regulations (Zha et al., 2010) as well as other hydro-climate and soil conditions. Overall, the total ET in broad leaf forests is larger than that of coniferous forests due to a larger volume of evaporation and sublimation that can occur from their canopy interception as compared to the coniferous forests. It has been shown that coniferous forests in western Canada have significantly lower fraction of ET to precipitation rates (40%) than grasslands (88%) (Liu et al., 2003). The modeled actual ET displayed in Fig. 7a5–f5, is the sum of all major ET components such as actual evaporation from the soil, actual transpiration by plants, evaporation of the canopy interception, and sublimation of snow. Therefore, we attributed ET increases to larger rates of transpiration from post-wildfire landuse types (e.g., grasslands and shrublands), as well as soil water evaporation and increased snow sublimation in the annual ET estimates. In addition, previous research in this region has shown greater energy available for snow processes after wildfire, potentially leading to elevated ET losses (Burles and Boon, 2011). Despite the potential support for increased post-fire ET, our results primarily illustrate the dominance of the climate change scenarios in driving the ET response. Given that most research has shown reduced post-fire ET, it is notable that even under high severity wildfire scenarios and when compounded with climate change, our ET increased relative to the pre-fire period. Such a response will have important implications for the longer-term downstream water supply in affected catchments.

Finally, annual sediment and TOC yields increased significantly in all wildfire-affected subbasins, which was the anticipated outcome (e.g., Bladon et al., 2014; Silins et al., 2009). For moderate burns, sediment yields increased by > 500% (0.8–547 tons) for the RCP 2.6 scenario (Fig. 7b6), and by 173% to > 500% (0.8–805 tons) for the RCP 8.5 scenario (Fig. 7e6). In the case of severe burns, all annual sediment yield increases were > 500%, ranging between 1.2 and 1,364 tons for the RCP 2.6 scenario (Fig. 7c6) and 1.3–1,421 tons by subbasin for the RCP 8.5 scenario (Fig. 7e6). Soil erodibility was among the least

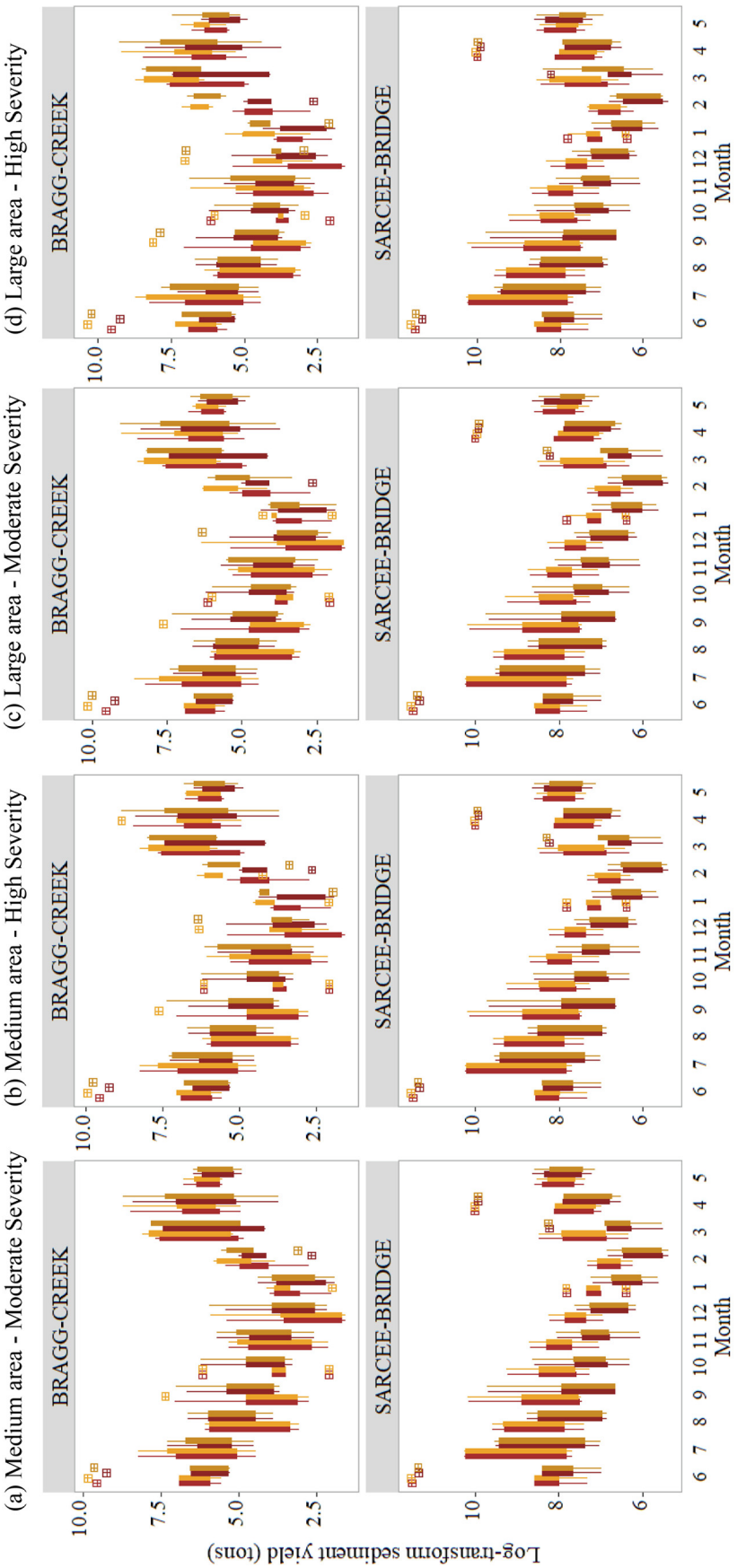

Fig. 9. Post-wildfire sediment yield (log-scale) at Bragg Creek and Sarcee Bridge for June 1st (month 6) wildfire in the five simulation years (2026, 2027, 2028, 2030, and 2032), and four wildfire scenarios: (a) medium area – moderate burn severity; b) medium area – high severity; (c) large area – moderate severity; (d) large area, high severity. The ranges illustrated by box plots are based on the annual variabilities in the five simulation years.

sensitive input parameters in the model affecting sediment yield during the calibration process (Du et al., 2020), and it increased according to wildfire severity (Table 2). Therefore, we hypothesized that surface runoff was the main driver of sediment transport in the model, which is in agreement with the modified universal soil loss equation (MUSLE) used in SWAT (Neitsch et al., 2011; Williams, 1995). For moderate burns, annual TOC yields increased by 76% to over 500% (123–163,900 kg) by subbasin for the RCP 2.6 scenario (Fig. 7b7), and by 84% to over 500% (115–165,900 kg) for the RCP 8.5 scenario (Fig. 7e7). For severe burns, increases ranged from 227% to over 500% (166–270,400 kg) for the RCP 2.6 scenario (Fig. 7c7), and from 392% to over 500% (173–278,600 kg) for the RCP 8.5 scenario (Fig. 7f7). The initial soil OC content remained the same for wildfire simulations, further supporting the hypothesis that erosion caused by surface runoff was also an important driver for TOC export. Furthermore, the most sensitive parameter that influenced simulated TOC was the POC enrichment ratio (Du et al., 2020), which determines how much POC sorbs to fine clay particles that are preferentially displaced by surface runoff.

3.4.2. Regional changes in streamflow

In the first year after wildfire, monthly streamflow at both Bragg Creek (mid watershed) and Sarcee Bridge (watershed outlet) stations increased in all wildfire scenarios, with changes most pronounced for the RCP 8.5 scenarios compared to the RCP 2.6 scenarios (Fig. 8). For RCP 2.6 scenarios, total annual streamflow at Sarcee Bridge was calculated by averaging changes in monthly streamflow, and only increased by 0.8%, 1.1%, 0.7%, and 1.9% for the medium-moderate, medium–high, large-moderate, and large-high burn scenarios, respectively. For the RCP 8.5 scenarios, annual streamflow, calculated by averaging changes in monthly streamflow, increased by 7.7%, 8.1%, 7.9%, and 9.3%, respectively. Annual streamflow increases during the first year after wildfire were greater in magnitude at the Bragg Creek station compared to that of Sarcee Bridge in all cases due to burn areas making up a larger proportion of drainage area for Bragg Creek relative to that of Sarcee Bridge (e.g., Moody et al., 2013).

Generally, streamflow increased in the 10 months that followed wildfires relative to the non-wildfire simulations (Fig. 8). Intensified streamflow resulted from greater runoff in the wildfire-affected subbasins, highlighting the importance of the forested regions in regulating water yield in the ER watershed. However, streamflow was lower during April and May, followed by a sharp relative increase in February and March, relative to non-wildfire simulations. This likely resulted from removal of the tree canopy, which would otherwise intercept snowfall during the winter (e.g., February and March) and moderate snow accumulation on the ground, as any form of precipitation that is intercepted by the tree canopy in SWAT evaporates or sublimates before precipitation that has made it to the ground surface (Neitsch et al., 2011). As well, the removal of shading from trees increases snow exposure to solar radiation, thus accelerating snowmelt in February and March, and leaving less snow for melting in April and May. Due to the proximity of Bragg Creek to the wildfire perimeter, relative increases in streamflow were greater compared to the Sarcee Bridge station. For all wildfire simulations, the RCP 8.5 climate change scenario showed a higher increase in streamflow than the RCP 2.6 scenario, due to more extreme precipitation and higher atmospheric CO_2, which can lower evapotranspiration rates (Deryng et al., 2016). Overall, annual streamflow at the ER watershed increased by a range of 0.7–9.3% for large area wildfire scenarios, in which 40% of total forest cover was lost, and replaced with grasslands or shrublands, and the wildfire perimeter encompassed approximately 20% of the entire watershed. The magnitude of these changes are comparable to SWAT model results of another study, in which annual streamflow increased by 2.4% after simulating the burning of 16% of a mountainous watershed in northern Spain (Morán-Tejeda et al., 2015). In the post-wildfire study in Colorado, minor changes in streamflow were observed at the watershed scale, because the wildfire location was near the watershed outlet rather than the headwater region and therefore streamflow impacts were minimal (Havel et al., 2018). Conversely, burned areas of the ER watershed were located at higher elevations where the majority of water originates, and therefore impacts of land cover changes were more pronounced.

3.4.3. Regional changes in sediments

As was anticipated based on other empirical studies using field measurements (e.g., Emelko et al., 2011; Writer et al., 2012), the monthly sediment yield in our study increased for all wildfire scenarios (Fig. 9). For the RCP 2.6 scenarios, the aggregated monthly data to annual sediment yield at Sarcee Bridge showed an increase of by 0.6%, 1.6%, 0.6% and 4.4% for the medium-moderate, medium–high, large-moderate, and large-high burn scenarios, respectively. Comparatively, for the RCP 8.5 scenarios, sediment yield increased by 1.2%, 2.4%, 1.9% and 6.5% for the medium-moderate, medium–high, large-moderate, and large-high burn scenarios, respectively. Sediment yield increases were higher at the Bragg Creek station compared to the Sarcee Bridge station (Fig. 8, Fig. 9). Although sediment yield by subbasin ranged between 173% to > 500% (Fig. 7), annual increases ranged from 25 to 193% at the Bragg Creek station, compared to only 0.6–6.5% at the Sarcee Bridge station. This is because Bragg Creek and Sarcee Bridge stations are over 10 km and 40 km downstream of wildfire-affected areas, respectively, and therefore model results are indicative of terrestrial and in-stream sediment deposition, as well as dilution on the way to the watershed outlet.

In another study area with similar characteristics to the ER watershed, Silins et al. (2009) determined from field-collected data that annual average TSS yields were 700% greater within streams of burned areas compared to non-burned areas. However, a key difference is that their water sampling sites were within the boundaries of the wildfire, and a larger proportion of the drainage area had burned. Water quality impacts depend on total area burned and its location within the watershed (Moody et al., 2013). Similar to the case of streamflow, relative changes were slightly greater for the medium–high scenario than the large-moderate scenario, suggesting that wildfire severity had a larger influence on erosion rates than the total area burned. Reduced sediment transport in the ER watershed model typically coincided with decreased streamflow in April and May at the Sarcee Bridge station (Figs. 8 and 9). The exception was slight decreases in August and October for the large-moderate and large-high scenarios, which are likely attributable to high sediment yields in prior months, which can lower availability of sediments for erosion from the landscape or within the stream; in other words, sediments that would otherwise settle and become available for resuspension, were instead transported out of subbasins by streamflow.

3.4.4. Regional changes in organic carbon

Wildfire simulations compounded with climate change typically resulted in higher TOC yields than climate change only scenarios, and all relative changes, whether increases or decreases, were greater in magnitude for the RCP 8.5 than the RCP 2.6 scenarios (Figs. 8 and 10). For the RCP 2.6 scenario, average annual TOC yield at Sarcee Bridge increased by 1.5–10.7% in the wildfire scenarios, and it changed within −1.1–19.7% range for the RCP 8.5 scenario. Similarly, the TOC yields at the Bragg Creek station increased −1.4–10.2% in the wildfire scenarios for the RCP 2.6 scenario, and it increased 0.5–16.1% for the RCP 8.5 scenario. In general, TOC yields were greater following the high severity scenarios, suggesting wildfire severity was a stronger driver of TOC than wildfire size, which is in agreement with findings of other studies (e.g., Abney et al., 2019). However, there was no statistical evidence ($p > 0.10$) for differences in the TOC yields from the wildfire scenarios compared to the climate change only scenarios, again suggesting that climate change may be a dominant driver of stream water chemistry. Empirical evidence has illustrated that post-fire carbon is highly variable and uncertain with observations of increases, decreases,

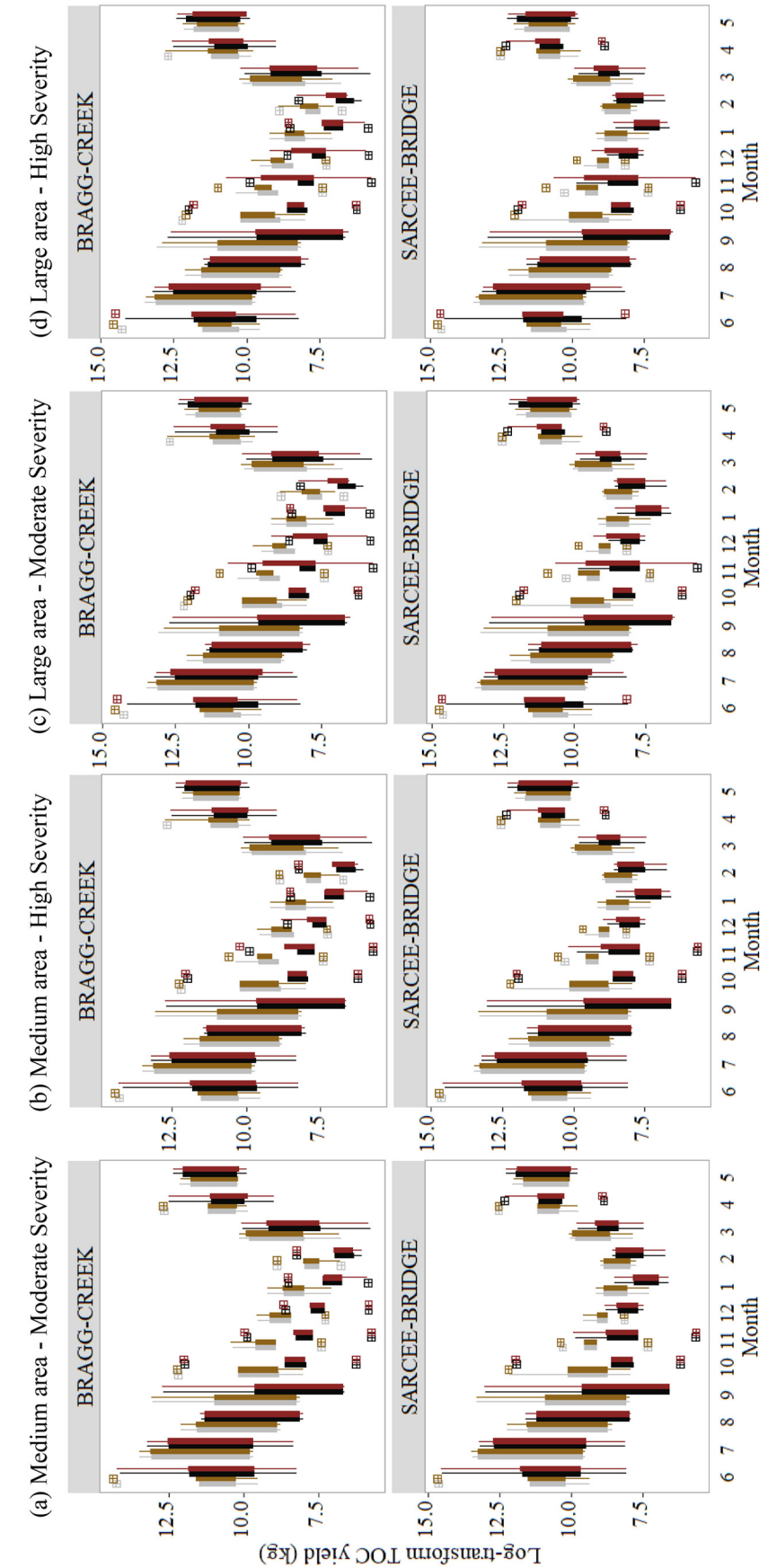

Fig. 10. Post-fire total organic carbon yield (log-scale) at Bragg Creek and Sarcee Bridge for June 1st (month 6) wildfire in years 2026, 2027, 2028, 2030, and 2032, and four wildfire scenarios: (a) medium area – moderate burn severity; b) medium area – high severity; (c) large area – moderate severity; (d) large area, high severity. The ranges illustrated by box plots are based on the annual variabilities in the five simulation years.

and no changes (Emelko et al., 2011; Hohner et al., 2019; Rhoades et al., 2019; Silins et al., 2009), and as such, it will be critical to continue to incorporate empirical data into future models to improve ability to model wildfire effects on this key water quality parameter.

All wildfire scenarios resulted in higher TOC yields in June (Fig. 8; month 6 in Fig. 10) than non-wildfire simulations. For the medium area wildfires, TOC yields generally increased in all months, with the exception of April and May (Fig. 8; month 4 and 5 in Fig. 10), due to earlier snowmelt and reduced surface runoff. Water from snowmelt is an important transport mechanism for OC (Writer et al., 2012), which our model captured in the month of March (Fig. 8; month 3 in Fig. 10). However, TOC yields at both stations decreased in July and August (Fig. 8; month 6–8 in Fig. 10) and early autumn for the large burn area scenarios, which contrasted field studies (e.g., Emelko et al., 2011; Writer et al., 2012). In a post-wildfire study of Fourmile Creek, a watershed in Colorado, USA, Writer et al. (2012) determined that in-stream DOC concentrations peaked during the first heavy precipitation event that followed the wildfire, and subsequent summer storms notably increased concentrations. After heavy rains, sediment and DOC levels remained elevated due to dissolution of POC, which underwent repeated deposition and resuspension within streams. As well, sediments in wildfire-affected areas are enriched in OC (Abney et al., 2019), and this was reflected in field data collected by Silins et al. (2009) for the Lost Creek wildfire. In the case of the ER watershed model, we hypothesized that post-wildfire rainstorms in June and snowmelt stripped the top soil layer of OC, and that this deficit led to lower TOC yields in subsequent months, despite the storm scenarios that were reflected by climate change induced precipitation scenarios. This is because our post-wildfire model inputs did not reflect plant debris, ash and incomplete combustion products, which can act as important sources of OC (e.g., Abney et al., 2019; Smith et al., 2011). In November (Fig. 8; month 11 in Fig. 10), TOC yields increased substantially for all wildfire simulations, and these changes were most significant for the high burn severity scenarios. We believe that the OC available for export increased in November because of the addition of plant residue in autumn, which marks the end of the growing season in SWAT-OCSM, thereby accounting for falling leaves and the death of seasonal plants and replenishing the soil OC supply through decomposition (Zhang et al., 2013).

4. Limitations and future directions

As it was not possible to calibrate our model under wildfire scenarios, we compared results to studies in other locations (e.g., Havel et al., 2018; Writer et al., 2012). Based on these correlations, the approach developed herein was determined to be a substantial step towards simulating impacts of potential wildfires. Notwithstanding this progress made, further improvements could be incorporated into future work. In post-wildfire parameterization, for the ER watershed, the SWAT-OCSM model assumed uniform burning within wildfire perimeters, whereas burn severity is often heterogeneous and based on factors such as elevation and aspect (e.g., Rogeau and Armstrong, 2017). Therefore, allowing patches of trees to remain with default soil parameters could create burn scenarios that are more realistic. This approach would maintain a proportion of canopy protection from rainfall, in addition to intercepting a portion of surface runoff and the transport of water quality constituents. Additionally, post-wildfire parameters within the model remained static, when in reality they would change with time. As an example, while relative changes in soil erodibility (Moody and Martin, 2009) and hydraulic conductivity (Ebel and Moody, 2017) can linger for several years after a wildfire, they typically diminish over longer time. As well, plant debris and ash accumulate after wildfires, and can be transported to streams by surface runoff, decreasing water quality for several years following wildfires (e.g., Smith et al., 2011). Since the initial terrestrial OC sources in our model were soil content and plant residues (Zhang et al., 2013), in-stream TOC was elevated for a short period following wildfire simulations, during which a large proportion of soil OC was removed by surface runoff during post-wildfire rain events. This occurred more quickly than plant residue could replenish the OC supply in the model, and therefore relative in-stream TOC levels decreased for several months afterwards relative to non-wildfire simulations, when they would be expected to remain elevated (e.g., Emelko et al., 2011; Writer et al., 2012). Therefore, we propose the addition of highly erodible and low-density soil layer with elevated TOC content that gradually erodes with storms (e.g., Doerr et al., 2009). Additionally, it would be beneficial for SWAT-OCSM to differentiate between different OC compounds such as pyrogenic carbon, which acts as a sorbent for organic matter and can remain within watersheds for decades (Abney et al., 2019). In addition, the current study used standard SWAT model water temperature module, which simplifies streamflow temperature (Ficklin et al., 2012; Giles et al., 2019), which may affect reaction and interaction rates of POC and DOC in SWAT-OCSM. Therefore, it would be useful to improve existing temperature simulation algorithm in the model for a more reliable prediction results. Finally, since impacts can persist for years, additional scenarios such as tree planting or natural succession could provide a long-term perspective on the impacts of wildfires on watersheds.

As our study area ended at the reservoir inlet (Fig. 1), this research did not address processes within the reservoir such as deposition of particulate matter or biological nutrient consumption. However, during peak runoff in June, water can be turbid throughout the reservoir (personal observation), and therefore it is likely that both POC and DOC can be present in larger quantities, increasing the need for coagulant and potentially creating harmful disinfection by-products through water treatment processes.

Although many researchers have collected post-wildfire field data (e.g., Abney et al., 2019; Cotrufo et al., 2016; Ebel and Moody, 2017; Emelko et al., 2011; Silins et al., 2009; Writer et al., 2012), relevant pre-wildfire data rarely exist for the same study areas due to the unpredictability of wildfire occurrences. Furthermore, responses to wildfire are highly variable, both between watersheds and within a single wildfire boundary, as they are affected by properties such as soil, vegetation, topography, climate, and burn severity (e.g., Plaza-Álvarez et al., 2018; Smith et al., 2011). The previous statements highlight the necessity for environmental monitoring in various watersheds in order to establish baseline conditions. This could include the installment of climate stations, hydrometric stations, or the collection of soil and water quality samples, which provide valuable data for identifying key environmental changes that result from extreme weather events, human activity, climate change, or any combination thereof.

5. Conclusion

Earlier studies lack a systematic assessment of the effects of climate change combined with discrete disturbance events, such as wildfires, on both water quantity and water quality by linking terrestrial and in-stream processes at the watershed scale. As such, this study aimed to assess the potential response of hydrological processes and streamflow, sediment yield, and organic carbon to wildfires and climate change scenarios in both terrestrial landscapes and in the streams. A process-based SWAT Organic Carbon Simulation Module (SWAT-OCSM) that integrates terrestrial and in-stream biogeochemical processes, was recently developed and used for analyses of this study. The main conclusions of this study are as follows:

- Our model suggests that both water quantity and quality could decrease in the future due to climate change. Reduced streamflow may occur due to lower overall precipitation and higher temperatures producing higher rates of evapotranspiration and earlier spring snowmelt.
- Intensified precipitation events may accelerate erosion, particularly

for the RCP 8.5 scenario. On average, in-stream sediment yields declined under climate change scenarios. However, higher erosion rates increase sediment available for transport during storms through resuspension, which can cause higher sediment fluxes for individual events. Suspended sediments can also facilitate the dissolution of organic matter attached to the sediment particles.

- Decreases in annual TOC yields were less than decreases in streamflow in the near and distant future compared to the baseline period. Since streamflow decline was significantly greater than TOC, a poorer water quality was projected for both future periods, particularly in the near future, due to a higher suspended POC, and higher DOC concentrations.
- Our model suggested that in the near future, high temperatures may lead to faster POC dissolution rates relative to DOC. Compounded with a significantly lower summer streamflow in this period, a higher overall concentration of OC will likely diminish the quality of water entering the reservoir at the watershed outlet.
- When compounded with wildfires, the climate change scenarios suggested higher streamflow, sediment yields, and TOC yields due to increased surface runoff relative to non-wildfire RCP simulations. However, the climate change scenarios remained the dominant driver of the hydrologic and water quality responses. This, in part, illustrated the challenges associated with modeling wildfire scenarios with most current hydrologic models. Given that wildfire regimes are shifting in many key source water regions, we suggest that future efforts continue to explore ways to develop more robust wildfire modules, reflecting post-fire changes in vegetation interception and transpiration, soil erodibility (USLE K factor), and surface and subsurface soil hydraulic properties (e.g., K_{sat}, Manning's n).
- Much of the sediment and TOC yielded from wildfire-affected subbasins did not reach the watershed outlet reservoir due to in-stream deposition. However, increasingly extreme precipitation events can ultimately reduce downstream water quality through increased sediment and nutrient export, particularly for high severity burns.
- Due to the sporadic nature of wildfires, opportunities to compare pre-wildfire and post-wildfire conditions are rare. Field data spanning a diversity of landscapes and climatic regimes are an important precursor to scenario analyses and future projections, particularly in the case of extreme events and disturbances, which can have almost immediate impacts on water quality. The methodology developed herein has the potential to be developed for use at a larger scale and within other watersheds to help facilitate risk assessments and development of forest and watershed management plans to mitigate risks.

Credit authorship contribution statement

Danielle Loiselle: Data curation, Formal analysis, Methodology, Software, Validation, Visualization, Writing - original draft, Writing - original draft. **Xinzhong Du:** Software, Writing - review & editing. **Daniel S. Alessi:** Conceptualization, Writing - review & editing. **Kevin D. Bladon:** Conceptualization, Writing - review & editing. **Monireh Faramarzi:** Supervision, Conceptualization, Formal analysis, Visualization, Writing - review & editing, Project administration, Funding acquisition.

Declaration of Competing Interest

The authors declare that they have no known competing financial interests or personal relationships that could have appeared to influence the work reported in this paper.

Acknowledgements

Funding for this study was primarily provided by Campus Alberta Innovation Program Chair (Grant #RES0034497), and Natural Sciences and Engineering Research Council of Canada Discovery (Grant #RES0043463). Time spent reviewing the paper by one of the co-authors was supported by the National Institute of Food and Agriculture, U.S. Department of Agriculture, McIntire Stennis project #1009768. We would like to thank the City of Calgary for providing water quality data.

Appendix A. Supplementary data

Supplementary data to this article can be found online at https://doi.org/10.1016/j.jhydrol.2020.125403.

References

Abney, R.B., Kuhn, T.J., Chow, A., Hockaday, W., Fogel, M.L., Berhe, A.A., 2019. Pyrogenic carbon erosion after the Rim Fire, Yosemite National Park: the role of burn severity and slope. J. Geophys. Res. Biogeosci. 124 (2), 432–449. https://doi.org/10.1029/2018jg004787.

Alberta Wildfire, 2019. accessed May 2019, < https://wildfire.alberta.ca/resources/historical-data/historical-wildfire-database.aspx > .

Ammar, M.E., Gharib, A., Islam, Z., Davies, E.G.R., Seneka, M., Faramarzi, M., 2020. Future floods using hydroclimatic simulations and peaks over threshold: an alternative to nonstationary analysis inferred from trend tests. Adv. Water Resour. 136, 103463. https://doi.org/10.1016/j.advwatres.2019.103463.

Arnold, J.G., Fohrer, N., 2005. SWAT2000: current capabilities and research opportunities in applied watershed modeling. Hydrol. Process. 19 (3), 563–572. https://doi.org/10.1002/hyp.56.

Azari, M., Saghafian, B., Moradi, H.R., Faramarzi, M., 2017. Effectiveness of soil and water conservation practices under climate change in the Gorganroud Basin. Iran: Soil Clean - Soil, Air, Water 45 (8), 1700288. https://doi.org/10.1002/clen.201700288.

Balfour, V.N., Doerr, S.H., Robichaud, P.R., 2014. The temporal evolution of wildfire ash and implicationsfor post-fire infiltration. Int. J. Wildland Fire 23, 733–745. https://doi.org/10.1071/WF13159.

Bart, R.R., 2016. A regional estimate of postfire streamflow change in California: a regional estimate of postfire streamflow change. Water Resour. Res. 52 (2), 1465–1478. https://doi.org/10.1002/2014wr016553.

Bladon, K.D., Emelko, M.B., Silins, U., Stone, M., 2014. Wildfire and the future of water supply. Environ. Sci. Technol. 48 (16), 8936–8943. https://doi.org/10.1021/es500130g.

Blount, K., Ruybal, C.J., Franz, K.J., Hogue, T.S., 2019. Increased water yield and altered water partitioning follow wildfire in a forested catchment in the western U.S. Ecohydrology e2170. https://doi.org/10.1002/eco.2170.

Bosch, J.M., Hewlett, J.D., 1982. A review of catchment experiments to determine the effect of vegetation changes on water yield and evapotranspiration. J. Hydrol. 55 (1-4), 3–23. https://doi.org/10.1016/0022-1694(82)90117-2.

Burles, K., Boon, S., 2011. Snowmelt energy balance in a burned forest plot, Crowsnest Pass, Alberta, Canada. Hydrol. Process. 25, 3012–3029. https://doi.org/10.1002/hyp.8067.

Cannon, A.J., 2015. Selecting GCM scenarios that span the range of changes in a multimodel ensemble: application to cmip5 climate extremes indices. J. Clim. 28, 1260–1267. https://doi.org/10.1175/JCLI-D-14-00636.1.

Cawley, K.M., Hohner, A.K., McKee, G.A., Borch, T., Omur-Ozbek, P., Oropeza, J., Rosario-Ortiz, F.L., 2018. Characterization and spatial distribution of particulate and soluble carbon and nitrogen from wildfire-impacted sediments. J. Soils Sediments 18 (4), 1314–1326. https://doi.org/10.1007/s11368-016-1604-1.

Chen, J., Chang, H., 2019. Dynamics of wet-season turbidity in relation to precipitation, discharge, and land cover in three urbanizing watersheds, Oregon. River Res. Appl. 35 (7), 892–904. https://doi.org/10.1002/rra.3487.

Chen, J., Brissette, F.P., Leconte, R., 2011. Uncertainty of downscaling method in quantifying the impact of climate change on hydrology. J. Hydrol. 401 (3-4), 190–202. https://doi.org/10.1016/j.jhydrol.2011.02.020.

Coogan, S.C.P., Robinne, F.-N., Jain, P., Flannigan, M.D., 2019. Scientists' warning on wildfire — a Canadian perspective. Can. J. For. Res. 49 (9), 1015–1023. https://doi.org/10.1139/cjfr-2019-0094.

Cotrufo, M.F., Boot, C.M., Kampf, S., Nelson, P.A., Brogan, D.J., Covino, T., Haddix, M.L., MacDonald, L.H., Rathburn, S., Ryan-Bukett, S., Schmeer, S., Hall, E., 2016. Redistribution of pyrogenic carbon from hillslopes to stream corridors following a large montane wildfire. Global Biogeochem. Cycles 30 (9), 1348–1355. https://doi.org/10.1002/2016GB005467.Received.

Cumming, S.G., 2001. FOREST type and wildfire in the Alberta boreal mixedwood: what do fires burn? Ecol. Appl. 11 (1), 97–110.

Deryng, D., Elliott, J., Folberth, C., Müller, C., Pugh, T.A.M., Boote, K.J., Conway, D., Ruane, A.C., Gerten, D., Jones, J.W., Khabarov, N., Olin, S., Schaphoff, S., Schmid, E., Yang, H., Rosenzweig, C., 2016. Regional disparities in the beneficial effects of rising CO2 concentrations on crop water productivity. Nat. Clim. Change 6 (8), 786–790. https://doi.org/10.1038/nclimate2995.

Doerr, S.H., Woods, S.W., Martin, D.A., Casimiro, M., 2009. 'Natural background' soil water repellency in conifer forests of the north-western USA: its prediction and relationship to wildfire occurrence. J. Hydrol. 371 (1-4), 12–21. https://doi.org/10.1016/j.jhydrol.2009.03.011.

Du, X., Loiselle, D., Alessi, D.S., Faramarzi, M., 2020. Hydro-climate and biogeochemical processes control watershed organic carbon inflows: development of an in-stream organic carbon module coupled with a process-based hydrologic model. Sci. Total Environ. 718, 137281. https://doi.org/10.1016/j.scitotenv.2020.137281.

Dutta, S., Sen, D., 2018. Application of SWAT model for predicting soil erosion and sediment yield. Sustain. Water Resour. Manage. https://doi.org/10.1007/s40899-017-0127-2.

Ebel, B.A., Moody, J.A., 2017. Synthesis of soil-hydraulic properties and infiltration timescales in wildfire-affected soils: synthesis of soil-hydraulic properties in wildfire-affected soils. Hydrol. Process. 31 (2), 324–340. https://doi.org/10.1002/hyp.10998.

Emelko, M.B., Silins, U., Bladon, K.D., Stone, M., 2011. Implications of land disturbance on drinking water treatability in a changing climate: demonstrating the need for "source water supply and protection" strategies. Water Res. 45 (2), 461–472. https://doi.org/10.1016/j.watres.2010.08.051.

Fabre, C., Sauvage, S., Tananaev, N., Noël, G.E., Teisserenc, R., Probst, J.L., Pérez, J.M.S., 2019. Assessment of sediment and organic carbon exports into the Arctic ocean: the case of the Yenisei River basin. Water Res. 158, 118–135. https://doi.org/10.1016/j.watres.2019.04.018.

Faramarzi, M., Abbaspour, K.C., Schulin, R., Yang, H., 2009. Modelling blue and green water resources availability in Iran. Hydrol. Process. 23, 486–501.

Faramarzi, M., Srinivasan, R., Iravani, M., Bladon, K.D., Abbaspour, K.C., Zehnder, A.J.B., Goss, G., 2015. Setting up a hydrological model of Alberta: data discrimination procedure prior to calibration. Environ. Modell. Software 74, 48–65.

Faramarzi, M., Abbaspour, K.C., Adamowicz, W.L., Lu, W., Fennell, J., Zehnder, A.J.B., Goss, G.G., 2017. Uncertainty based assessment of dynamic freshwater scarcity in semi-arid watersheds of Alberta, Canada. J. Hydrol.: Reg. Stud. 9, 48–68.

Farjad, B., Gupta, A., Marceau, D.J., 2016. Annual and seasonal variations of hydrological processes under climate change scenarios in two sub-catchments of a complex watershed. Water Resour. Manage. 30 (8), 2851–2865. https://doi.org/10.1007/s11269-016-1329-3.

Ficklin, D.L., Luo, Y., Stewart, I.T., Maurer, E.P., 2012. Development and application of a hydroclimatological stream temperature model within the Soil and Water Assessment Tool. Water Resour. Res. 48 (1), W01511. https://doi.org/10.1029/2011WR011256.

Fischer, H., Sachse, A., Steinberg, C.E.W., Pusch, M., 2002. Differential retention and utilization of dissolved organic carbon by bacteria in river sediments. Limnol. Oceanogr. 47 (6), 1702–1711. https://doi.org/10.4319/lo.2002.47.6.1702.

Flannigan, M.D., Logan, K.A., Amiro, B.D., Skinner, W.R., Stocks, B.J., 2005. Future Area Burned in Canada. Clim. Change 72 (1-2), 1–16. https://doi.org/10.1007/s10584-005-5935-y.

Gartner, J.E., Cannon, S.H., Santi, P.M., Dewolfe, V.G., 2008. Empirical models to predict the volumes of debris flows generated by recently burned basins in the western U.S. Geomorphology 96 (3-4), 339–354. https://doi.org/10.1016/j.geomorph.2007.02.033.

Gassman, P.W., Arnold, J.G., Srinivasan, R., Reyes, M., 2010. The worldwide use of the SWAT model: technical drivers, networking impacts, and simulation trends. In: Proceeding of 21st Century Watershed Technology: Improving Water Quality and Environment, CD-Rom Proceedings, 21e24 February 2010, Costa Rica.

Giles, N.A., Babbar-Sebens, M., Srinivasan, R., Ficklin, D.L., Barnhart, B., 2019. Optimization of linear stream temperature model parameters in the soil and water assessment tool for the continental United States. Ecol. Eng. 127, 125–134. https://doi.org/10.1016/j.ecoleng.2018.11.012.

Hallema, D.W., Sun, G.e., Caldwell, P.V., Norman, S.P., Cohen, E.C., Liu, Y., Bladon, K.D., McNulty, S.G., 2018. Burned forests impact water supplies. Nat. Commun. 9. https://doi.org/10.1038/s41467-018-03735-6.

Havel, A., Tasdighi, A., Arabi, M., 2018. Assessing the long-term hydrologic response to wildfires in mountainous regions. Hydrol. Earth Syst. Sci. 22 (25), 2527–2550. https://doi.org/10.5194/hess-2017-604.

Hernandez, A.J., Healey, S.P., Huang, H., Ramsey, R.D., 2018. Improved prediction of stream flow based on updating land cover maps with remotely sensed forest change detection. Forests 9 (6), 1–19. https://doi.org/10.3390/f9060317.

Hohner, A.K., Terry, L.G., Townsend, E.B., Summers, R.S., Rosario-Ortiz, F.L., 2017. Water treatment process evaluation of wildfire-affected sediment leachates. Environ. Sci. Water Res. Technol. 3 (2), 352–365. https://doi.org/10.1039/c6ew00247a.

Hohner, A.K., Rhoades, C.C., Wilkerson, P., Rosario-Ortiz, F.L., 2019. Wildfires alter forest watersheds and threaten drinking water quality. Acc. Chem. Res. 52, 1234–1244. https://doi.org/10.1021/acs.accounts.8b00670.

Hudson, J.A., Crane, S.B., Blackie, J.R., 1997. The Plynlimon water balance 1969–1995: the impact of forest and moorland vegetation on evaporation and stream flow in upland catchments. Hydrol. Earth Syst. Sci. 1, 409–427. https://doi.org/10.5194/hess-1-409-1997.

IPCC, 2013. Climate Change 2013: The Physical Science Basis. Contribution of Working Group I to the Fifth Assessment Report of the Intergovernmental Panel on Climate Change. Cambridge University Press, Cambridge, United Kingdom and New York, NY, USA, pp. 1535.

Iravani, M., White, S.R., Farr, D.R., Habib, T.J., Kariyeva, J., Faramarzi, M., 2019. Assessing the provision of carbon-related ecosystem services across a range of temperate grassland systems in western Canada. Sci. Total Environ. 680, 151–168. https://doi.org/10.1016/j.scitotenv.2019.05.083.

James, A.L., Roulet, N.T., 2007. Investigating hydrologic connectivity and its association with threshold change in runoff response in a temperate forested watershed. Hydrol. Process. 21 (25), 3391–3408. https://doi.org/10.1002/hyp.6554.

Jepsen, S.M., Harmon, T.C., Sadro, S., Reid, B., Chandra, S., 2019. Water residence time (age) and flow path exert synchronous effects on annual characteristics of dissolved organic carbon in terrestrial runoff. Sci. Total Environ. 656, 1223–1237. https://doi.org/10.1016/j.scitotenv.2018.11.392.

Jung, H.Y., Hogue, T.S., Rademacher, L.K., Meixner, T., 2009. Impact of wildfire on source water contributions in Devil Creek, CA: evidence from end-member mixing analysis. Hydrol. Process. 23 (2), 183–200. https://doi.org/10.1002/hyp.7132.

Keeley, J.E., 2009. Fire intensity, fire severity and burn severity: a brief reviewand suggested usage. Int. J. Wildland Fire 18, 116–126. https://doi.org/10.1071/WF07049.

Keenan, T.F., Hollinger, D.Y., Bohrer, G., Dragoni, D., Munger, J.W., Schmid, H.P., Richardson, A.D., 2013. Increase in forest water-use efficiency as atmospheric carbon dioxide concentrations rise. Nature 499https://doi.org/10.1038/nature12291. 324-+.

Kelliher, F.M., Leuning, R., Schulze, E.D., 1993. Evaporation and canopy characteristics of coniferous forests and grasslands. Oecologia 95 (2), 153–163. https://doi.org/10.1007/BF00323485.

Kemanian, A.R., Julich, S., Manoranjan, V.S., Arnold, J.R., 2011. Integrating soil carbon cycling with that of nitrogen and phosphorus in the watershed model SWAT: theory and model testing. Ecol. Model. 222 (12), 1913–1921. https://doi.org/10.1016/j.ecolmodel.2011.03.017.

Kirby, C., Newson, M. D., Gilman, K. 1991 Plynlimon Research: The First Two Decades. Institute of Hydrology Report No. 109, Wallingford, UK, p. 188. Available from: < http://nora.nerc.ac.uk/6052/1/IH_109.pdf > .

Krysanova, V., White, M., 2015. Advances in water resources assessment with SWAT: an overview. Hydrol. Sci. J. 60 (5), 771–783. https://doi.org/10.1080/02626667.2015.1029482.

Kulig, J.C., Edge, D., Reimer, W., Bill, Townshend, I., Lightfoot, N., 2009. Levels of risk: perspectives from the lost creek fire. Aust. J. Emergency Manage. 24 (2), 33–39.

Larsen, S., Andersen, T., Hessen, D.O., 2011. Climate change predicted to cause severe increase of organic carbon in lakes. Global Change Biol. 17 (2), 1186–1192. https://doi.org/10.1111/j.1365-2486.2010.02257.x.

Laudon, H., Buttle, J., Carey, S.K., McDonnell, J., McGuire, K., Seibert, J., Shanley, J., Soulsby, C., Tetzlaff, D., 2012. Cross-regional prediction of long-term trajectory of stream water DOC response to climate change. Geophys. Res. Lett. 39 (18), 4–9. https://doi.org/10.1029/2012GL053033.

Leppi, J.C., DeLuca, T.H., Harrar, S.W., Running, S.W., 2012. Impacts of climate change on August stream discharge in the Central-Rocky Mountains. Clim. Change 112 (3-4), 997–1014. https://doi.org/10.1007/s10584-011-0235-1.

Lessels, J.S., Tetzlaff, D., Carey, S.K., Smith, P., Soulsby, C., 2015. A coupled hydrology-biogeochemistry model to simulate dissolved organic carbon exports from a permafrost-influenced catchment: a coupled hydrology-biogeochemistry model. Hydrol. Process. 29 (26), 5383–5396. https://doi.org/10.1002/hyp.10566.

Liu, J., Chen, J.M., Cihlar, J., 2003. Mapping evpotraspiration based on remote sensing: an application to Canada's landmass. Water Resour. Res. 39 (7), 1189. https://doi.org/10.1029/2002WR001680.

Mahat, V., Silins, U., Anderson, A., 2016. Effects of wildfire on the catchment hydrology in southwest Alberta. Catena 147, 51–60. https://doi.org/10.1016/j.catena.2016.06.040.

Malagó, A., Bouraoui, F., Vigiak, O., Grizzetti, B., Pastori, M., 2017. Modelling water and nutrient fluxes in the Danube River Basin with SWAT. Sci. Total Environ. 603-604, 196–218. https://doi.org/10.1016/j.scitotenv.2017.05.242.

Marlon, J.R., Bartlein, P.J., Gavin, D.G., Long, C.J., Anderson, R.S., Briles, C.E., Brown, K.J., Colombaroli, D., Hallett, D.J., Power, M.J., Scharf, E.A., Walsh, M.K., 2012. Long-term perspective on wildfires in the western USA. Proc. Natl. Acad. Sci. 109 (9), 3203–3204. https://doi.org/10.1073/pnas.1112839109.

Masud, M.B., Ferdous, J., Faramarzi, M., 2018. Projected changes in hydrological variables in the agricultural region of Alberta, Canada. Water 12 (10). https://doi.org/10.3390/w10121810.

Masud, M.B., Wada, Y., Goss, G., Faramarzi, M., 2019. Global implications of regional grain production through virtual water trade. Sci. Total Environ. 659, 807–820. https://doi.org/10.1016/j.scitotenv.2018.12.392.

Meierdiercks, K.L., Smith, J.A., Baeck, M.L., Miller, A.J., 2010. Hetero-geneity of hydrologic response in urban watersheds. J. Am. Water Resour. Assoc. 46 (6), 1221–1237. https://doi.org/10.1111/j.1752-1688.2010.00487.x. CHEN AND CHANG903.

MirHadi Madani, E., Jansson, P.E., Babelon, i., 2018. Differences in water balance between grassland and forest watersheds using long-term data, derived using the CoupModel. Hydrol. Res. 49 (1), 72–89. https://doi.org/10.2166/nh.2017.154.

Monteith, J.L., 1965. Evaporation and the environment. In: The state and movement of water in living organisms. 19th symposia of the Society for Experimental Biology. Cambridge University Press, London, U.K, pp. 205–234.

Moody, John A., Martin, Deborah A., 2001. Post-fire, rainfall intensity-peak discharge relations for three mountainous watersheds in the western USA. Hydrol. Process. 15 (15), 2981–2993. https://doi.org/10.1002/hyp.386.

Moody, John A., Martin, Deborah A., 2009. Synthesis of sediment yields after wildland fire in different rainfall regimes in the western United States. Int. J. Wildland Fire 18 (1), 96. https://doi.org/10.1071/WF07162.

Moody, J.A., Shakesby, R.A., Robichaud, P.R., Cannon, S.H., Martin, D.A., 2013. Current research issues related to post-wildfire runoff and erosion processes. Earth Sci. Rev. 122, 10–37. https://doi.org/10.1016/j.earscirev.2013.03.004.

Morán-Tejeda, E., Zabalza, J., Rahman, K., Gago-Silva, A., López-Moreno, J.I., Vicente-Serrano, S., Lehmann, A., Tague, C.L., Beniston, M., 2015. Hydrological impacts of climate and land-use changes in a mountain watershed: uncertainty estimation based on model comparison: hydrological impacts of environmental change in a mountain watershed. Ecohydrol. 8 (8), 1396–1416. https://doi.org/10.1002/eco.1590.

Moriasi, D.N., Gitau, M.W., Pai, N., Daggupati, P., 2015. Hydrologic and water quality models: performance measures and evaluation criteria. Trans. ASABE 58 (6),

1763–1785. https://doi.org/10.13031/trans.58.10715.
Nalley, J.O., O'Donnell, D.R., Litchman, E., 2018. Temperature effects on growth rates and fatty acid content in freshwater algae and cyanobacteria. Algal Res. 35, 500–507. https://doi.org/10.1016/j.algal.2018.09.018.
Neitsch, S.L., Arnold, J.G., Kiniry, J.R., Williams, J.R., 2011. Soil and Water Assessment Tool Theoretical Documentation Version 2009. Texas Water Resources Institute.
Newson, M.D., 1985. Twenty years of catchment process studies: what have we taught the engineer. In: Advances in Water Engineering. Elsevier, London UK, pp. 39–46.
Ni, X., Parajuli, P.B., 2018. Evaluation of the impacts of BMPs and tailwater recovery system on surface and groundwater using satellite imagery and SWAT reservoir function. Agric. Water Manag. 210, 78–87.
Niemeyer, R.J., Bladon, K.D., Woodsmith, R.D., 2020. Long-term hydrologic recovery after wildfire and post-fire forest management in the interior Pacific Northwest. Hydrol. Process. 34, 1182–1197. https://doi.org/10.1002/hyp.13665.
Osborn, G., Stockmal, G., Haspel, R., 2006. Emergence of the Canadian Rockies and adjacent plains: a comparison of physiography between end-of-Laramide time and the present day. Geomorphology 75 (3-4), 450–477. https://doi.org/10.1016/j.geomorph.2005.07.032.
Ozturk, I., Sharif, B., Baby, S., Jabloun, M., Olesen, J.E., 2018. Long-term simulation of temporal change of soil organic carbon in Denmark: comparison of three model performances under climate change. J Agric. Sci. 156, 139–150. https://doi.org/10.1017/S0021859617000971.
Parton, W.J., Rasmussen, P.E., 1994. Long-Term Effects of Crop Management in Wheat-Fallow: II. CENTURY Model Simulations. Soil Sci. Soc. Am. J. 530–536. https://doi.org/10.2136/sssaj1994.03615995005800020040x.
Plaza-Álvarez, P.A., Lucas-Borja, M.E., Sagra, J., Moya, D., Alfaro-Sánchez, R., González-Romero, J., De las Heras, J., 2018. Changes in soil water repellency after prescribed burnings in three different Mediterranean forest ecosystems. Sci. Total Environ. 644, 247–255. https://doi.org/10.1016/j.geomorph.2005.07.032.
Pomeroy, J.W., Gray, D.M., Brown, T., Hedstrom, N.R., Quinton, W.L., Granger, R.J., Carey, S.K., 2007. The cold regions hydrological model: a platform for basing process representation and model structure on physical evidence. Hydrol. Process. 21, 2650–2667. https://doi.org/10.1002/hyp.
Poon, P.K., Kinoshita, A.M., 2018. Spatial and temporal evapotranspiration trends after wildfire in semi-arid landscapes. J. Hydrol. 559, 71–83. https://doi.org/10.1016/j.jhydrol.2018.02.023.
Rhoades, C.C., Chow, A.T., Covino, T.P., Fegel, T.S., Pierson, D.N., Rhea, A.E., 2019. The legacy of a severe wildfire on stream nitrogen and carbon in headwater catchments. Ecosystems 22 (3), 643–657. https://doi.org/10.1007/s10021-018-0293-6.
Robichaud, P.R., Wagenbrenner, J.W., Pierson, F.B., Spaeth, K.E., Ashmun, L.E., Moffet, C.A., 2016. Infiltration and interrill erosion rates after a wildfire in western Montana, USA. Catena 142, 77–88. https://doi.org/10.1016/j.catena.2016.01.027.
Robinne, F.N., Bladon, K.D., Silins, U., Emelko, M.B., Flannigan, M.D., Parisien, M.A., Wang, X., Kienzle, S.W., Dupont, D.P., 2019. A regional-scale index for assessing the exposure of drinking-water sources to wildfires. Forests 10 (5), 1–21. https://doi.org/10.3390/f10050384.
Robinson, M., Dupeyrat, A., 2005. Effects of commercial timber harvesting on streamflow regimes in the Plynlimon catchments, mid-Wales. Hydrol. Process. 19, 1213–1226. https://doi.org/10.1002/hyp.5561.
Rodrigues, E.L., Jacobi, C.M., Figueira, J.E.C., 2019. Wildfires and their impact on the water supply of a large neotropical metropolis: a simulation approach. Sci. Total Environ. 651, 1261–1271. https://doi.org/10.1016/j.scitotenv.2018.09.289.
Rodríguez-Jeangros, N., Hering, A.S., McCray, J.E., 2018. Analysis of anthropogenic, climatological, and morphological influences on dissolved organic matter in Rocky Mountain streams. Water (Switzerland) 10 (4), 1–46. https://doi.org/10.3390/w10040534.
Rogeau, M.-P., Armstrong, G.W., 2017. Quantifying the effect of elevation and aspect on fire return intervals in the Canadian Rocky Mountains. For. Ecol. Manage. 384, 248–261. https://doi.org/10.1016/j.foreco.2016.10.035.
Rogeau, M.-P., Flannigan, M.D., Hawkes, B.C., Parisien, M.A., Arthur, R., 2016. Spatial and temporal variations of fire regimes in the Canadian Rocky Mountains and Foothills of southern Alberta. Int. J. Wildland Fire 25 (11), 1117. https://doi.org/10.1071/WF15120.
Rood, S.B., Pan, J., Gill, K.M., Franks, C.G., Samuelson, G.M., Shepherd, A., 2008. declining summer flows of Rocky Mountain rivers: changing seasonal hydrology and probable impacts on floodplain forests. J. Hydrol. 349 (3-4), 397–410. https://doi.org/10.1016/j.jhydrol.2007.11.012.
Rostami, S., He, J., Hassan, Q.K., 2018. Riverine water quality response to precipitation and its change. Environments 5 (1), 1–17. https://doi.org/10.3390/environments5010008.
Rust, A.J., Hogue, T.S., Saxe, S., McCray, J., 2018. Post-fire water-quality response in the western United States. Int. J. Wildland Fire 27 (3), 203–216. https://doi.org/10.1071/WF17115.
Seidl, R., Thom, D., Kautz, M., Martin-Benito, D., Peltoniemi, M., Vacchiano, G., Wild, J., Ascoli, D., Petr, M., Honkaniemi, J., Lexer, M.J., Trotsiuk, V., Mairota, P., Svoboda, M., Fabrika, M., Nagel, T.A., Reyer, C.P.O., 2017. Forest disturbances under climate change. Nat. Clim. Change 7 (6), 395–402. https://doi.org/10.1038/nclimate3303.
Shakesby, R.A., Bento, C.P.M., Ferreira, C.S.S., Ferreira, A.J.D., Stoof, C.R., Urbanek, E., Walsh, R.P.D., 2015. Impacts of prescribed fire on soil loss and soil quality: an assessment based on an experimentally-burned catchment in central Portugal. Catena 128, 278–293.
Shrestha, N.K., Wang, J., 2018. Predicting sediment yield and transport dynamics of a cold climate region watershed in changing climate. Sci. Total Environ. 625, 1030–1045. https://doi.org/10.1016/j.scitotenv.2017.12.347.
Silins, U., Stone, M., Emelko, M.B., Bladon, K.D., 2009. Sediment production following severe wildfire and post-fire salvage logging in the Rocky Mountain headwaters of the Oldman River Basin, Alberta. Catena 79 (3), 189–197. https://doi.org/10.1016/j.catena.2009.04.001.
Smith, H.G., Sheridan, G.J., Lane, P.N.J., Nyman, P., Haydon, S., 2011. Wildfire effects on water quality in forest catchments: a review with implications for water supply. J. Hydrol. 396 (1-2), 170–192. https://doi.org/10.1016/j.jhydrol.2010.10.043.
Son, K., Lin, L., Band, L., Owens, E.M., 2019. Modelling the interaction of climate, forest ecosystem, and hydrology to estimate catchment dissolved organic carbon export. Hydrol. Process. 33 (10), 1448–1464.
Townsend, S.A., Douglas, M.M., 2004. The effect of a wildfire on stream water quality and catchment water yield in a tropical savanna excluded from fire for 10 years (Kakadu National Park, North Australia). Water Res. 38 (13), 3051–3058. https://doi.org/10.1016/j.watres.2004.04.009.
Tuppad, P., Douglas-Mankin, K.R., Lee, T., Srinivasan, R., Arnold, J.G., 2011. Soil and Water Assessment Tool (SWAT) hydrologic/water quality model: extended capability and wider adoption. Trans. ASABE 54 (5), 1677–1684.
Wang, X., Thompson, D.K., Marshall, G.A., Tymstra, C., Carr, R., Flannigan, M.D., 2015. Increasing frequency of extreme fire weather in Canada with climate change. Clim. Change 130 (4), 573–586. https://doi.org/10.1007/s10584-015-1375-5.
Werner, A.T., Cannon, A.J., 2016. Hydrologic extremes - an intercomparison of multiple gridded statistical downscaling methods. Hydrol. Earth Syst. Sci. 20, 1483–1508. https://doi.org/10.5194/hess-20-1483-2016.
Williams, J.R., 1995. Chapter 25: The EPIC model. In: Singh, V.P. (Ed.), Computer Models of Watershed Hydrology. Water Resources Publications, pp. 909–1000.
Willmore, N. Jensen, H.G., 1960. Alberta's Forests, Government of the Province of Alberta, Department of Lands and Forests, Edmonton.
Wine, M L, Cadol, D., 2016. Hydrologic effects of large southwestern USA wildfires significantly increase regional water supply: fact or fiction? Environ. Res. Lett. 11 (8), 13. https://doi.org/10.1088/1748-9326/11/8/085006.
Worku, T., Khare, D., Tripathi, S.K., 2017. Modeling runoff–sediment response to land use/land cover changes using integrated GIS and SWAT model in the Beressa watershed. Environ. Earth Sci. 76 (16), 1–14. https://doi.org/10.1007/s12665-017-6883-3.
Writer, J.H., McCleskey, R.B., Murphy, S.F., 2012. Effects of wildfire on source-water quality and aquatic ecosystems, Colorado Front Range. In: Wildfire and Water Quality: Processes, Impacts, and Challenges. IAHS Publ, pp. 117–123.
Wu, Y., Ouyang, W., Hao, Z., Lin, C., Liu, H., Wang, Y., 2018. Assessment of soil erosion characteristics in response to temperature and precipitation in a freeze-thaw watershed. Geoderma 328, 56–65. https://doi.org/10.1016/j.geoderma.2018.05.007.
Yu, M., Bishop, T.F.A., Van Ogtrop, F.F., 2019. Assessment of the decadal impact of wildfire on water quality in forested catchments. Water (Switzerland) 11 (3), 1–17. https://doi.org/10.3390/w11030533.
Zha, T., Barr, A.G., van der Kamp, G., Black, T.A., McCaughey, J.H., Flanagan, L.B., 2010. Interannual variation of evapotranspiration from forest and grassland ecosystems in western canada in relation to drought. Agric. For. Meteorol. 150 (11), 1476–1484. https://doi.org/10.1016/j.agrformet.2010.08.003.
Zhang, X., Izaurralde, R.C., Arnold, J.G., Williams, J.R., Srinivasan, R., 2013. Modifying the Soil and Water Assessment Tool to simulate cropland carbon flux: model development and initial evaluation. Sci. Total Environ. 463-464, 810–822. https://doi.org/10.1016/j.scitotenv.2013.06.056.